



Society for Pediatric Pathologists
Abstracts of the 2021 Fall Meeting
October 8-9, 2021
Virtual Meeting

PLATFORM I: Placenta

1

Recurrence risk of villitis of unknown etiology: analysis of a large retrospective cohort study and systematic review

L de Koning¹, S Crawford², E Nohr³, J Wright, Jr¹, C Horn³, E Chan³

¹University of Calgary, Calgary, Alberta; ²Alberta Health Services, Calgary, Alberta; ³Alberta Precision Laboratories, Calgary, Alberta

Background: Recurrence risk of villitis of unknown etiology (VUE) remains uncertain due to heterogeneity of study characteristics such as criteria for placental examination, rule-out of infectious causes, pathologist specialization, and small numbers of initial and recurrent VUE cases. Further, few studies have expressed recurrence risk according to parity and gravida – which may help set ‘lower bounds’ on recurrence risk. Our first objective was to determine recurrence risk of VUE in a large population of placentas sent for pathologic examination by pediatric and perinatal pathologists at our institution using clearly defined and consistent criteria, and to express recurrence risk per parity and gravida. Our second objective was to compare these estimates to others from the literature via systematic review.

Methods: Eleven years (2010-2021) of placenta pathology reports on singleton pregnancies ≥ 20 weeks gestation in Calgary, Alberta, Canada were retrieved from the Cerner Millennium lab information system, and candidate reports with villitis were identified using a Perl script searching for ‘villitis’ or VUE’. Cases of acute villitis and chronic villitis due to infections were eliminated via pathologist review. Reports were merged to gestational age, parity and gravida from Alberta Perinatal Health Program data. VUE recurrence risk (among patients with ≥ 2 placentas examined) per patient, parity and gravida were determined. Results were compared to those found among articles and their references identified via an Ovid MEDLINE® (1946-June 2021) search using keywords for VUE and recurrence.

Results: We retrieved 29185 placenta pathology reports from 27146 patients. There were 2424 cases of VUE among 2383 patients (8.8% / patient, 4.9% per parity, and 3.7% per gravida). Among 153 patients who had ≥ 2 placentas examined, there were 41 recurrent cases (each only occurring once) of VUE for a recurrence risk of 27% per patient (22% / parity, 19% / gravida). The literature search identified 64 articles, of which 6 were retrieved for data extraction – 1 of which was a conference abstract cited by an article but not identified in the initial search. Reported recurrence risks per patient were 8-56%, with 9-575 initial cases of VUE, and 5-17 recurrent cases. One study, which examined all placentas from all births over a ~ 3 year period, also found a recurrence risk of 27%.

Conclusion: In our study, which is the largest of its kind to date, VUE recurrence risk was $\sim 27\%$. We feel that this result, while lower than in other studies, may better represent actual recurrence risk – especially if parity and gravida are considered.

Prevalence of chronic histiocytic intervillitis before and after the COVID-19 pandemic*S Ikegami¹, L Ernst²*¹University of Cincinnati, Department of Pathology, Cincinnati, Ohio; ²NorthShore University HealthSystem, Department of Pathology, Evanston, Illinois

Background: Various placental pathology has been described in association with the coronavirus disease 2019 (COVID-19) in pregnancy, but no distinctive pattern has emerged as specific. However, the pattern of chronic histiocytic intervillitis (CHI) with trophoblast necrosis may be associated with the most severe forms of COVID-19 in pregnancy. Our objective was to examine the prevalence of CHI pre and post COVID-19 pandemic and describe the patterns of pathology seen in severe acute respiratory syndrome coronavirus 2 (SARS-CoV-2) positive versus negative patients.

Methods: We searched our pathology database for the diagnosis of “chronic intervillitis” from 1/1/2017 to 6/1/2021. H&E slides were reviewed, and CHI categorized as “massive” (≥50% involvement) or focal (<50% involvement). We also collected demographic data from maternal and neonatal charts, including results of any SARS-CoV-2 testing. All statistics were computed using SPSS.

Results: A total of 19 CHI cases were identified in the study period, 7 in the three years prior to pandemic onset (1/1/2017-12/31/2019) and 12 in the 1.5 years after pandemic onset (1/1/2020-6/1/2021). In the post-pandemic group, 7/12 (58%) mothers with CHI tested positive and 3/12 (25%) tested negative for SARS-CoV-2. Two mothers had unknown SARS-CoV-2 infection status. Among 9 living children in the post-pandemic group, only one had a documented positive SARS-CoV-2 test result. Three (3/12, 25%) fetal deaths were noted in the post-pandemic group; two with unknown maternal SARS-CoV-2 test status and one in a mother with SARS-CoV-2 infection diagnosed 8 days before delivery. No fetal deaths were noted in the 7 patients with CHI pre-pandemic. In analysis excluding the two patients with unknown infection status, massive CHI was seen only in SARS-CoV-2 positive patients (4/7 SARS-CoV-2 positive vs 0/10 SARS-CoV-2 negative; $p=0.015$), and those same 4 patients also had massive perivillous fibrin deposition (MPVFD). SARS-CoV-2 positive patients with CHI all had positive testing within 36 days of delivery (mean 9.7 day, range 0-36 days) and the 4 cases with massive CHI were positive within 14 days of delivery (mean 7.25 days, range 0-14 days). There were no statistically significant differences in maternal age, gestational age at delivery, mode of delivery, birthweight and placental weight between positive and negative patients.

Conclusion: Massive CHI is a rare placental lesion, but has shown increased prevalence since the COVID-19 pandemic. In our small study, massive CHI was seen only post-pandemic and only in mothers testing positive for SARS-CoV-2. All cases of massive CHI were accompanied by MPVFD in our study, suggesting the combination of these two rare lesions may be a relatively specific finding in SARS-CoV-2 placental infection.

Examining the Impact of Villitis of Unknown Etiology Histopathological Lesion and Adverse Clinical Neonatal Outcomes in an Eastern Ontario Maternity Population

B Osborne¹, S Dancey², I Oltean³, V Bijelic⁴, S Lawrence⁵, F Moretti⁶, J de Nanassy³, S Bainbridge⁷, D El Demellawy³

¹Children's Hospital of Eastern Ontario Research Institute, Ottawa, Ontario; ²Faculty of Medicine, University of Ottawa, Ottawa, Ontario; ³Department of Pathology, Children's Hospital of Eastern Ontario, Ottawa, Ontario; ⁴Clinical Research Unit, Children's Hospital of Eastern Ontario, Ottawa, Ontario; ⁵Department of Pediatrics, Children's Hospital of Eastern Ontario, Ottawa, Ontario; ⁶Department of Obstetrics and Gynecology, The Ottawa Hospital, Ottawa, Ontario; ⁷Faculty of Health Sciences, University of Ottawa, Ottawa, Ontario

Background: Villitis of unknown etiology (VUE) is a histopathological lesion affecting 5-15% of term placentas. VUE has previously been linked to intrauterine growth restriction (IUGR), recurrent pregnancy loss, and neurological abnormalities in the newborn. The impact of VUE histopathology features, namely severity and distribution, remains unclear. We seek to define the relationship between VUE diagnosis (severity, distribution) and short-term adverse neonatal outcomes.

Methods: A retrospective chart review of placental pathology findings from placentas diagnosed with VUE from 2013-2016 at the Department of Pathology was conducted. Cases of VUE were identified by a search through electronic medical records. Placental pathology reports were examined to confirm the diagnosis of VUE and record severity and distribution according to the *Amsterdam Consensus Statement* criteria. Control placentas were randomly selected, matching based on gestational age at delivery (+/- 1 week) and fetal IUGR status. Cases of multiple gestation were excluded from the analysis. Neonatal outcomes of interest include: need for newborn resuscitation, neonatal intensive care unit (NICU) admission, APGAR scores (at 1 and 5 minutes) and cord pH. Data are presented as median (IQR) for continuous and frequency (%) for categorical variables. Odds ratios (OR) and 95% confidence intervals (CIs) were calculated with the control cases as the reference group.

Results: 226 placentas with VUE, and 232 control placentas without VUE were identified after matching and excluding multiple gestations. Across the entire cohort, the median gestational age was 38 weeks [36-39]. 35% of total placentas were complicated by IUGR. When analysed by severity (low-grade: OR = 4.75 [2.86-8.14], $p < 0.001$; high-grade: OR = 4.76 [2.71-8.79], $p < 0.001$) and distribution (focal: OR = 5.24 [2.87-10.17], $p < 0.001$; multifocal: OR = 4.90 [2.90-8.59], $p < 0.001$), both the severity and distribution of VUE lesions were significantly associated with the need for newborn resuscitation. None of the other neonatal outcomes of interest were significantly associated with the severity or distribution of VUE.

Conclusion: We determined a marked increase in the need for newborn resuscitation in placentas demonstrating VUE, which loosely supports a possible relationship between placental dysfunction and this outcome. Further study is needed to indicate whether VUE histopathology features are correlated with the level of invasiveness of newborn resuscitation when required. VUE severity and distribution were not associated with any additional neonatal outcomes of interest. Additional studies with larger sample sizes are required to confirm the absence of these associations for obstetric and neonatal care providers.

SARS-CoV-2 Infection of the Placenta Should not be Called "SARS-CoV-2 Placentitis", a Term that is Misleading, Not Supported by the Literature, and Should be Abandoned: A Review of the Literature of Chronic Histiocytic Intervillositis

M Luquette

University of Minnesota, Department of Pathology, Minneapolis, Minnesota

Background: Chronic Histiocytic Intervillositis (CHI) is a pattern of inflammation in the placenta that was first described 34 years ago and has been heavily reported in the last 2 years in cases of maternal Covid-19 infection with vertical transmission across the placenta. CHI has been reported in placentas of patients with malaria, CMV, and autoimmune conditions affecting the placenta, including pedigrees in which fetus specific antibodies target HLA mismatched paternal haplotypes. With an increase in reports using the term "SARS-CoV-2 Placentitis" (SCP) and the referencing of reports that use the term, the question arises, "Is there any evidence that CHI is caused by SARS-CoV-2" thus justifying the term SCP.

Methods: To date 122 articles are returned in a PubMed search of "Intervillositis". Full text of these articles was downloaded and the articles were reviewed and data recorded for: year of publication; journal type; a pathologist as an author; type of study; conclusions; reporting of incidence of CHI; type of intervillositis; reporting of gravidity and parity; Covid-19 as a topic; claims that SARS-CoV-2 causes CHI; mention of vertical transmission, an autoimmune process, or trophoblast necrosis; and claims that the Ace2 receptor is a portal of infection. Data were reviewed to answer the above stated question.

Results: There were 4 articles that used the term SARS-CoV-2 placentitis, 1 with SARS-CoV-2 inflammation, and 1 with SARS-CoV-2 intervillositis. While some of these studies ruled out some viral infections, they do not adequately assess autoimmunity as an etiology for CHI in the reported cases. Seven articles claim either primary viral infection of the trophoblast or that the virus causes CHI. They do not contemplate that the damage may be a mixture of primary autoimmune damage followed by additional damage by SARS-CoV-2 or that a non-covid cause may be the initiator of the CHI. Four studies reporting incidence of CHI in placentas > 36 weeks gestation, pre-covid, show an incidence of 0.098 to 0.4%. Two studies of incidence of CHI (not in the intervillositis search) in placentas > 37 weeks gestation, post-covid, show an incidence of 0-0.27%. No data is reported showing an increased incidence in CHI, post-covid.

Conclusion: While CHI can easily be appreciated as a portal for placental infection by SARS-CoV-2 that may well magnify trophoblast necrosis beyond what is normally seen in CHI, there is nothing in the literature that proves that CHI or a Covid modified version of CHI is initiated by SARS-CoV-2 vs another etiology, namely an autoimmune condition. Hence the term "SARS-CoV-2 Placentitis" and similar terms are misleading and should be abandoned. Issuing separate diagnoses of CHI and SARS-CoV-2 infection is recommended.

Placental Histopathology Associated with SARS-CoV-2 Infection in Pregnancy: Preliminary Data from a Prospective Cohort Study in Ontario, Canada

S Fellus¹, S Dancey¹, Y Nasr², S Mohammad³, G Vasam³, S Bainbridge⁴, S Girard⁵, B de Vrijer⁶, A Dingwall Harvey³, R Fakhraei³, M Murphy³, D El-Chaâr³, D El-Demellawy⁷

¹Faculty of Medicine, University of Ottawa, Ottawa, Ontario; ²Faculty of Science, University of Ottawa, Ottawa, Ontario; ³Clinical Epidemiology Program, Ottawa Hospital Research Institute, Ottawa, Ontario; ⁴Faculty of Health Sciences, University of Ottawa, Ottawa, Ontario; ⁵Department of Obstetrics and Gynecology, Université de Montréal, Montreal, Quebec; ⁶Department of Obstetrics and Gynaecology, Western University, London; ⁷Department of Paediatric Pathology, Children's Hospital of Eastern Ontario, Ottawa, Ontario

Background: Severe acute respiratory syndrome coronavirus 2 (SARS-CoV-2) has been responsible for significant maternal and neonatal morbidity. Examination of placentas from individuals infected with SARS-CoV-2 during pregnancy have demonstrated maternal vascular malperfusion, fetal vascular malperfusion and evidence of inflammation, however studies to date are limited by small sample sizes, paucity of information on maternal comorbidities, and lack of data about infection time point. The objective of this study was to investigate placental findings of cases compared to controls, as well as to compare recovered versus active cases at the time of delivery.

Methods: This was a sub-study of a large multi-center prospective cohort study of pregnant women with clinically-confirmed SARS-CoV-2 infection in Ontario, Canada, from March-July 2021. Placentas collected from study participants delivering at a single site were used for this preliminary analysis. Demographic and clinical (i.e., preeclampsia, gestational diabetes, chronic diabetes, and intrauterine growth restriction) data were extracted from patient medical records. Placentas were evaluated for frequency and type of histologic lesions using a placental phenotypic classification tool (Freedman et al., 2021). Findings from cases were compared to those from pregnancies not complicated by SARS-CoV-2. Timing of infection in pregnancy was also considered. Fisher's exact test was used for comparing categorical data. Continuous data was compared using a 2-sample t-test.

Results: A total of 47 women had placental samples available for this analysis, including 33 cases and 14 controls. Among the cases, 8 (24.2%) were positive for SARS-CoV-2 infection at delivery and 25 (75.8%) were recovered from infections earlier in pregnancy. Six (18.2%) cases and 3 (21.4%) controls had comorbidities in pregnancy. The mean gestational age and standard deviation at delivery was 39.06±2.12 weeks, and 7 (21.2%) cases delivered by C-section compared to 7 (50%) of controls. Placental pathology of individuals infected in pregnancy did not differ compared to controls. Individuals infected with SARS-CoV-2 at the time of delivery did not have different rates of placental lesions compared to those infected earlier in pregnancy.

Conclusion: In this preliminary analysis we conducted histopathological examinations of placentas from women testing positive for SARS-CoV-2 at any time point during pregnancy as well as from women who had tested negative. Cases and controls had similar rates of placental lesions. Timing of infection did not significantly impact placental pathology. Analysis of the full cohort, including controls matched for gestational age and comorbidities, is forthcoming in order to more robustly assess placental pathology in pregnant women infected with SARS-CoV-2.

Intervillositis in Placentas from Gestations Complicated by Maternal SARS-CoV-2 Infection: Fetal and Neonatal Outcomes

J Havens¹, O Faye-Petersen¹, A Lu², A Feldman¹, V Duncan¹, N Arora²

¹The University of Alabama at Birmingham Department of Pathology, Birmingham, Alabama; ²The University of Alabama at Birmingham Department of Pediatrics, Birmingham, Alabama

Background: Most placentas from SARS-Cov-2 positive mothers are normal or reflect nonspecific pathology. Intervillositis is a severe but rare pattern of injury recently described in placentas of mothers with SARS-CoV-2 infection. Relationships of this pathology to SARS-CoV-2 infection, fetal and neonatal outcomes, and maternal symptomatology are poorly understood.

Methods: We report a series of placentas from 6 SARS-CoV-2 positive women collected 3/2020-8/2021. Gestational age ranged from 22-37 weeks. Placental tissue was collected, stained, and evaluated using standard protocols. In situ hybridization (ISH) specific for SARS-CoV-2 S gene encoding the spike protein was performed on paraffin-embedded tissue.

Results: All placentas showed intervillositis accompanied by trophoblast necrosis and variable perivillous fibrinoid deposition. In 5 cases, the inflammation was predominantly monocytic; one case had mixed inflammation with a predominant neutrophilic component. No cases showed significant villitis. The pathology was diffuse in 4 cases and patchy but widespread in 2 cases. All cases showed strong positive ISH staining of the villous trophoblast in a circumferential perivillous pattern. All maternal infections were acute, within about 2 weeks prior to delivery. Outcomes included intrauterine fetal demise in 2 cases and neonatal demise in 1 case. All 3 had diffuse placental inflammation, but all were also complicated by either severe chronic uteroplacental pathology or clinical circumstances preventing emergent delivery. Three babies survived. One baby had low Apgar scores and extended intensive care unit care, and had only patchy placental inflammation. One baby had initial low Apgar scores and metabolic acidosis with diffuse placental involvement. One baby (the only baby born at term) had patchy placental inflammation and did well. All of the liveborn neonates had negative tests at birth for SARS-CoV-2; the term neonate had a subsequent positive test. Maternal symptomatology varied and did not appear to relate to fetal or neonatal outcome.

Conclusion: This series, though small, supports an association between placental intervillositis and maternal SARS-CoV-2. Degree of placental compromise is likely an important determinant in fetal/neonatal outcome. However, despite severe placental pathology, mortality in this series occurred only in the setting of comorbid complications, suggesting that timing of delivery and close maternal monitoring is important in mitigating poor outcomes. Further studies are needed to investigate the associations of this rare but severe pattern of placental injury.

Recurrence of placental lesions in a pathology sample

A Freedman¹, L Ernst²

¹Northwestern University, Evanston, Illinois; ²NorthShore University HealthSystem, Evanston, Illinois

Background: Several placental lesions are known to recur in subsequent pregnancies. However, estimates of recurrence are often based on risk, which does not include a comparison group. A comparison group, as included in the risk ratio, helps to account for the baseline prevalence of the lesion in the sample, which can be affected by differences in the underlying population, indications for pathologic review, and sampling techniques. Our goal was to estimate the recurrence risk ratio for the major placental lesion categories.

Methods: The study sample included placentas submitted for pathologic review at a single hospital between January 2009 and March 2018. During the study period, 21,917 patients had two deliveries and 883 patients had placental pathology reports available for both deliveries. Pathology reports were completed by perinatal pathologists and placental lesions were classified based on Amsterdam consensus criteria: acute placental inflammation (API), chronic placental inflammation (CPI), maternal vascular malperfusion (MVM), and fetal vascular malperfusion (FVM). Log-binomial models were used to estimate recurrence risk ratios for the four major placental lesion categories. Models were adjusted for maternal and pregnancy characteristics, including race/ethnicity, interpregnancy interval, and maternal age and parity at the time of the first study pregnancy. Inverse probability weights were used to partially account for selection into the pathology sample.

Results: In our pathology-based sample, the prevalence of recurrent pathology was 27.0% for API, 22.5% for CPI, 21.7% for MVM, and 12.2% for FVM. The recurrence risk ratio (RR) was strongest for CPI, indicating that those with CPI in the first pregnancy were 1.61 times as likely to develop CPI in the subsequent pregnancy as compared to those without CPI in the first pregnancy (95% confidence interval [CI]: 1.40, 1.84). Similarly, those with MVM in the first pregnancy were 1.55 times as likely to develop MVM in the subsequent pregnancy (95% CI: 1.29, 1.86) and those with FVM in the first pregnancy were 1.23 times as likely to develop FVM in the subsequent pregnancy (95% CI: 1.04, 1.44). API in the first pregnancy was not associated with API in the subsequent pregnancy after controlling for covariates and accounting for selection bias (RR: 1.10; 95% CI: 0.95, 1.27).

Conclusion: Our results suggest that CPI, MVM, and FVM may recur in a subsequent pregnancy, even after controlling for covariates and partially accounting for selection bias. We did not observe evidence of recurrence for API. Additional research is needed to understand recurrence risk in a representative sample, to evaluate whether grade of pathology is important, and to explore whether specific lesions are driving recurrence estimates.

Impact of Co-existing Placental Pathologies in Pregnancies complicated by Placental Abruption and Acute Neonatal Outcomes

I Oltean¹, D Mavedatnia², J Tran², V Bijelić¹, S Lawrence³, D El Demellawy³

¹Children's Hospital of Eastern Ontario Research Institute, Ottawa, Ontario; ²University of Ottawa School of Medicine, Ottawa, Ontario; ³Children's Hospital of Eastern Ontario, Ottawa, Ontario

Background: Placental abruption (PA) is a critical concern for maternal and neonatal morbidity and mortality. Adverse perinatal outcomes in the setting of PA, include higher risk of fetal-growth restriction, stillbirth, prematurity, and birth asphyxia. Placental pathologies as defined by the Amsterdam consensus include maternal vascular malperfusion (MVM), fetal vascular malperfusion (FVM), acute chorioamnionitis, and villitis of unknown etiology (VUE), among others. These pathologies are independently associated with the presence of perinatal complications. The aim of this present study is to investigate if placental pathologies can adversely affect acute neonatal outcome in pregnancies complicated with PA.

Methods: A retrospective cohort study was conducted. All placentas with the pathologic or clinical diagnosis of PA and/or retroplacental hematoma from October 1st 2013 to April 30th 2020 were identified from the pathology archives using Epic-Hyperspace. A clinical diagnosis of abruption was confirmed via ultrasound or the clinical presentation of vaginal bleeding, abdominal pain, uterine contractions, or uterine tenderness, as defined on the electronic medical records (EMRs). The pathological diagnosis was then confirmed post-delivery with placental examination for the presence of MVM, FVM, acute chorioamnionitis and VUE. The presence of retroplacental clot(s) were also assessed as additional coexisting pathologies. Our outcomes were NICU admission, BD 10-15.9 or BD \geq 16, cord pH \leq 7 or 7.1-7.15, Apgar score at 10-minutes \leq 5, need for resuscitation, and small-for-gestational age. The effect of placental pathology on NICU admission and other outcomes were investigated using logistic regression analysis. Two-sided P-values less than 0.05 and odds ratios (ORs) with 95% confidence intervals (CI) excluding one, denoted statistical significance.

Results: A total of 287 placentas were identified. There were 110 (38%) of placentas with PA alone vs 177 (62%) with placental abruption and additional placental pathologies. Odds of NICU admission were more than two times higher in pregnancies with placental pathologies [OR=2.15, 95% CI 1.21, 3.90; p-value = 0.01]. Odds of Apgar score \leq 5 was more than four times higher among pregnancies with placental pathologies [OR=4.56, 95% CI 1.28-21.26; p-value = 0.03].

Conclusion: Our study shows that a coexisting placental pathology(ies) may impact acute neonatal outcomes, notably NICU admission and Apgar scores in pregnancies complicated by PA. Exploration of potential clinical confounders to examine this relationship in detail, is warranted.

PLATFORM II: Perinatal and Pediatric

9

Prior cesarean section correlates with higher invasiveness grade in patients with Placenta Accreta Spectrum: Questioning the concept of uterine scar dehiscence

G Neville, A Sharma, C Parra-Harran

Brigham and Women's Hospital, Boston, Massachusetts

Background: Placenta accreta spectrum disorders (PAS) are an increasingly common obstetric challenge associated with significant maternal morbidity and mortality. Recent guidelines have established that the diagnosis and classification of PAS on hysterectomy material requires distinction between placental tissue at the site of scar dehiscence and true myometrial invasion. It remains uncertain whether such distinction can be made on histologic examination and whether it is clinically important.

Methods: The aim of this study was to establish differences between PAS associated with a cesarean section (CS) scar or prior instrumentation and PAS without such a history. We retrieved slides from gravid hysterectomies with a diagnosis of PAS in our institution. Each case was reviewed along with obstetric history and clinical outcomes. PAS grade was assigned following recent recommendations (PMID: 32415266). A trichrome stain was applied to all cases to aid in this assessment.

Results: Of 61 histologically confirmed PAS cases, 80.3% (n=49) had a history of prior CS. Of the remaining, 13.1% (n=8) had a history of uterine instrumentation, whereas 6.6% (n=4) had no prior history of CS or uterine instrumentation (one had undergone in vitro fertilization (IVF)). Of those with a history of prior CS, most (n=42, 85.7%) had the placental bed in the anterior lower uterine segment (area of the prior CS scar). Six of the 7 remaining cases had a prior hysteroscopic resection for retained production of conception. Patients with prior CS section were significantly more likely to present with advanced PAS grade: 28.6% (n=14) were grade 1, 12.2% (n=6) were grade 2, 20.4% (n=10) were grade 3a and 38.8% (n=19) were grade 3D. In contrast, of those with prior instrumentation per PAS grading system; 62.5% (n=5) were grade 1, 25% (n=2) were grade 2 and 12.5% (n=1) 3a. Of those with no prior instrumentation or CS per PAS grading system; 50% (n=2) were grade 1, 25% (n=1) were grade 2 and 25% (n=1) were grade 3d. Fisher's t-test confirmed a significantly higher PAS grade in the CS group compared to other PAS cases ($p^* < 0.05$). Placenta previa was only documented in PAS with history of CS (n=27, 55%) or uterine instrumentation (n=3, 37.5%).

Conclusion: Clear risk factors are present in most patients with PAS with just 4.9% (n=3) lacking history of prior uterine surgery or IVF. Importantly, previous CS is associated with a higher PAS grade suggesting that placental invasiveness is not restricted to the myometrium but also affects, and is even facilitated by, the previous CS scar anatomy. The distinction between scar dehiscence and true myometrial invasion is difficult but its refinement may allow improved correlation between grading and clinical significance.

Association of Placental Pathology with Growth Arrest Line Formation in Fetal Growth Restriction*T Chu, W Parks, P Shannon*

University of Toronto, Toronto, Ontario

Background: Asymmetric fetal growth restriction (GR) is a common consequence of severe gestational uterine and placental pathology. Although bone shortening and irregular growth are a hallmark of GR, there are no systematic studies correlating bone growth with placental pathology. In this study, we examine the relationship between growth arrest lines (GAL) and placental pathology in a large cohort of pathologically investigated cases of fetal asymmetrical GR.

Methods: We used text word searching of our laboratory information system to identify all fetal or neonatal autopsies demonstrating growth arrest lines or growth restriction over a period of 5/12 years. Each case was reviewed for the severity of growth restriction and associated pathologies. We excluded cases of symmetrical growth restriction, aneuploidy, multiple congenital anomalies, and multiple pregnancies. The accompanying uteroplacental, and umbilical cord pathologies were reviewed and categorized as placental pathologies (maternal vascular malperfusion, fetal vascular malperfusion, significant intervillous or subchorial haematoma, chronic villitis, intervillitis, perivillous fibrinoid deposition, delayed villous maturation., placenta accreta spectrum) or umbilical cord pathology (abnormalities of coiling, insertion or thrombosis). Associated histology of whole mounted long bone growth arrest lines was also retrieved.

Results: We searched 2,108 fetal post mortems, and retrieved 112 cases of non-syndromic, isolated asymmetrical growth restriction. Of these, 16 (14%) had growth arrest lines. 5 further cases had GAL without GR. In asymmetric GR, GAL were associated with a wide variety of placental diseases, but most commonly with fetal and maternal vascular malperfusion. The presence of GAL did not correlate with the severity of the GR, nor were GAL associated with specific placental pathologies. 5 histologically demonstrated cases of GAL in asymmetric GR were retrieved: all showed (from epiphysis towards metaphysis) subchondral radiodensity, followed by a zone of radiolucency, followed by a zone of radiodensity. The radiolucency corresponds to a zone of poor trabecular bone formation, with the sclerotic zone in the metaphysis to coarse trabeculae with poor remodeling.

Conclusion: GAR are thought to represent episodic severe slowing of fetal growth; however, we found GAL in the presence of placental pathologies usually thought to be steadily progressive (e.g. maternal vascular malperfusion, histiocytic intervillitis). Further the histological pattern is not that of a simple period of slow growth. We conclude that GAL can accompany a wide variety of placental diseases, but that their biology is poorly understood.

Fetal Vascular Ectasia Can Be an Artifact of Placental Fixation

P Katzman, L Metlay

University of Rochester Medical Center, Rochester, New York

Background: As part of our perinatal pathology service, our institution processes placentas from multiple outlying hospitals. In contrast to in-house placentas, these placentas are formalin-fixed en route to our laboratory. We identified that the chorionic, stem villus, and umbilical vessels in these fixed placentas are often ectatic in a greater frequency than in our in-house fresh placentas. In order to identify whether fixation was associated with this increased rate of vascular ectasia, we fixed all our incoming in-house placentas for a period of time to compare with these outside cases.

Methods: We searched our LIS for third trimester placentas using the keywords “ectasia” or “ectatic” over a period of 12 months. We also fixed all incoming in-house placentas over a two-week period for approximately 24-72 hours and tabulated fixation time and the presence or absence of ectasia of chorionic, stem villus, and umbilical vessels, as defined by Parast et al, 2008, as vascular distension to at least four times the diameter of an adjacent muscular vessel of similar caliber. Statistical comparisons were performed using www.medcalc.org.

Results: The LIS search identified 51/83 (61%) of placental cases from outlying hospitals that had ectatic vessels versus 56/2110 (3%) in in-house placentas ($p < 0.0001$). Of the 38 placentas fixed in a two week period, 17 (45%) had ectatic chorionic or stem villus vessels and 8 (21%) had umbilical vessel ectasia. 6/38 (16%) had ectasia in both umbilical and chorionic/stem villus vessels. In comparison, in the two subsequent weeks, 3.8% (2/52) ($p < 0.0001$) of fresh placentas had vascular ectasia.

Conclusion: These data suggest that large fetal vessels in the placenta become engorged with blood at the time of delivery and, if fixed soon after delivery, remain ectatic and congested when processed for pathology. When placentas remain unfixed prior to prosection, these vessels have time to drain and deflate. The identification of this artifactual ectasia is important because fetal vessel ectasia can suggest the presence of fetal vascular malperfusion if other signs of this entity are present, such as vascular organizing thrombi, avascular/sclerotic villi, and villous stromal-vascular karyorrhexis.

Congenital Cytomegalovirus (CMV) Infection But Negative Second Trimester Maternal CMV IgM Antibodies – A Report of 4 Cases

E Chan¹, H Zhou²

¹University of Calgary, Calgary, Alberta; ²Alberta Precision Laboratories, Calgary, Alberta

Background: Congenital cytomegalovirus (cCMV) is the most common congenitally acquired viral infection. Pregnant women are not routinely tested for CMV infection; maternal CMV IgG/IgM testing typically occurs following suspicious prenatal ultrasound (US) findings. The diagnosis of a recent CMV infection is often considered less likely if CMV IgM is -ve.

Methods: We described 4 cases of cCMV infection with placental and/or autopsy findings, in which the 2nd trimester maternal CMV IgM was -ve.

Results: **Case 1.** A 20-year-old (yo) G2P0 woman presented with prenatal US findings suggestive of intrauterine infection at 24 1/7 weeks gestational age (GA). Maternal CMV IgG/IgM performed at 25 weeks GA were +ve and -ve respectively. Placental examination following fetal demise at 30 3/7 weeks GA revealed CMV-associated villitis. **Case 2.** A 26 yo G2P0 woman with fetal hydrops diagnosed at 19 5/7 weeks GA had CMV testing at 21 1/7 weeks GA; IgG was +ve and IgM was -ve. At 21 6/7 weeks, amniotic fluid CMV PCR was +ve. In light of this finding, CMV IgG avidity was performed on the 21 1/7 weeks GA maternal blood sample and it showed low avidity. Placental examination following termination of pregnancy (TOP) at 24 4/7 weeks GA confirmed cCMV. **Case 3.** A 39 yo G1P0 woman presented with simple fetal ascites at 19 2/7 weeks GA. Maternal CMV IgG was +ve and IgM was -ve at 19 3/7 weeks GA. TOP due to fetal intracranial bleed occurred at 22 weeks GA. Autopsy/placental examination revealed cCMV. Subsequently, CMV serologies performed on the mother's stored blood sample from 11 4/7 weeks GA demonstrated +ve IgM and low IgG avidity, suggesting maternal CMV infection around the time of conception. **Case 4.** A 33 yo G4P2 woman whose prenatal US at 20 4/7 weeks GA showed mildly increased abdominal circumference had c-section at 26 weeks GA for abruption. At the time of delivery, maternal CMV IgG was +ve and IgM was -ve. The baby had respiratory distress and thrombocytopenia, and died on day 5 of life. Autopsy revealed diffuse CMV infection. Testing performed on the mother's stored prenatal blood sample (collected at 9 5/7 weeks GA) demonstrated +ve CMV IgG/IgM and low IgG avidity, indicating maternal CMV infection around the time of conception.

Conclusion: In each of these 4 cases, maternal CMV IgM performed in 2nd trimester was -ve; thus, cCMV infection was not originally suspected. Yet, autopsy and/or placental examination demonstrated CMV infection in all 4 cases. In 2 of these cases, stored maternal blood samples from 1st trimester demonstrated +ve CMV IgG, +ve IgM, and low IgG avidity, confirming maternal CMV infection around the time of conception. These cases illustrated that CMV IgM response can be short-lived; thus, cCMV should not be ruled out based on a -ve maternal CMV IgM result in 2nd or 3rd trimester.

Pulmonary Complications after Bone Marrow Transplantation at a large Pediatric Institution.

N Cortes-Santiago¹, J Pogoriler², K Patel¹, S Sartain¹, M Silva-Carmona¹, S Bhar¹, G Deutsch³

¹Texas Children's Hospital, Baylor College of Medicine, Houston, Texas; ²Children's Hospital of Philadelphia, Philadelphia, Pennsylvania; ³Seattle Children's Hospital, Seattle, Washington

Background: Physiology and pathologic features of non-infectious post-BMT pulmonary complications are poorly understood making interpretation of lung biopsies challenging in this patient population. In this study, we characterize the primary lung pathologic findings in 30 post-BMT patients at a large pediatric hospital with correlation to patient's clinical course and clinical suspicion of pulmonary complications, including graft-versus-host disease (GVHD) and idiopathic pneumonia syndrome (IPS).

Methods: Pathology database was queried from 2009-2019 to identify post-BMT patients who had undergone lung biopsy or lung transplantation. Electronic medical record was reviewed for pertinent clinical and demographic data. Pathology material was reviewed by two pathologists (NCS and GD). Findings related to airway and airspace disease, interstitial disease, vasculopathic changes and infectious processes were documented. Primary disease process was classified according to aggregate clinical-pathologic data.

Results: Thirty patients met inclusion criteria: median age, 14.4 yrs (10 mo – 24.6 yrs), M:F ratio, 2:1, median age at BMT, 12.8 yrs (7 mo - 24.2 yrs) and median post-BMT interval at biopsy, 7 months (8 d–11 yrs). Reasons for BMT were malignant (17) and benign (12) hematologic and metastatic medulloblastoma (1). BMT types were 1 autologous, 7 matched related donor (MRD), 10 matched unrelated donor (MUD), 4 mismatched RD (MMRD) and 8 MMUD. At the time of this study, 18 patients were deceased, 9 alive and 3 were lost to follow up. Death occurred at a median of 49 days after biopsy (6-102 d). Seven of 18 patients with available information received total body irradiation. Clinical impression was infectious in most cases (18); others were GVHD (3), cryptogenic organizing pneumonia (1) and unknown or undetermined (8), one of which had a diagnosis of IPS. Pathologic findings included bronchiolitis obliterans in 5 of 23 (22%) adequate cases, including 2 explants. Vasculopathic changes were seen in 25 of 28 (89%) adequate cases. Three major pathologic classifications were noted: infectious (12), GVHD (5) and likely toxicity (9); 4 remained of unclear etiology. Clinicopathologic concordance was 30%, all infectious. Five of the 8 patients with unknown clinical diagnosis were deemed to be likely toxic injury on pathologic exam. Biopsy led to change in management in 9 of 17 (53%) patients with available information.

Conclusion: Infection continues to be a major cause of morbidity and mortality post-BMT. Vasculopathic changes are exceedingly common, presumably related to drug/radiation toxicity. This argues for a significant role of vascular injury in non-infectious post-BMT pulmonary complications, particularly in those patients with an unclear clinical picture including those with a diagnosis of IPS.

Comparing Temperature-Controlled and Direct-to-Freezer Cryopreservation on Cell Viability and PDX Engraftment in Wilms Tumor

L Rutherford¹, T Bhat², V Chow¹, S Vercauteren¹, C Lim², J Bush¹

¹BC Children's and Women's Hospital, Vancouver, British Columbia; ²BC Children's Hospital Research Institute, Vancouver, British Columbia

Background: Pediatric malignant solid tumors are typically triaged in the fresh state into multiple potential pathways, which may include formalin-fixation, touch preparations, snap-freezing, and glutaraldehyde. These methods provide adequate clinical diagnostic information, but are not typically amenable to establishing cell lines or patient-derived xenografts (PDXs). This could serve as a limitation at both the bench and bedside as more clinical and research studies have moved towards personalized medicine. Additionally, cryopreservation is often associated as needing specialized temperature-controlled freezing apparatuses, which may provide a barrier to adoption. We sought to test various types of cryopreservation media and dissociation methods using Wilms tumor (WT) as a tumor model through post-thaw cell counts and chorioallantoic membrane (CAM) xenograft success.

Methods: Fresh WT tissue was processed for cryopreservation and freezing at -80C using four methods: 2 x 3mm chunks in 10% DMSO, 2 x 3mm chunks in CELLBANKER 2 (CB2, Amsbio LLC) freezing media, single cells dissociated by density-gradient separation in 10% DMSO, and single cells dissociated using GentleMACs dissociator in 10% DMSO. After four weeks, the samples were thawed and the chunks frozen in 10% DMSO and CB2 were dissociated into single cells. Cell counts were obtained from all samples and tumour spheroids were prepared from dissociated cells by mixing cell suspension and Matrigel in 1:1 ratio and incubated overnight before implantation. Matrigel encapsulated cells were on-planted into the chicken CAM model to assess tumour growth. Ethics approval was obtained.

Results: By day three, all four methods showed tumour growth in the CAM, with the GentleMACs and density-gradient methods of dissociation exhibiting an objectively fuller looking tumour mass than the other methods. By day six, growth expansion plateaued and day nine was the final day of imaging and termination of the CAM model. PDXs were harvested on days 5 and 6 for future cryopreservation and for histologic examination.

Conclusion: The use of CB2 for cryopreservation showed no inferiority to 10% DMSO in terms of cell viability nor CAM expansion. Dissociation of tissues into single cells pre-freeze displayed no marked advantage to tumour growth in CAM compared to freezing in chunks. Our findings would suggest the use of either a temperature-controlled method (10% DMSO) or direct-to-freezer method (CB2) for cryopreservation, and that additional pre-freeze preparation by dissociation does not effect viability or growth in Wilms tumor. These pilot results may support the use of CB2 at pathology sites that would not significantly impact fresh-tissue triaging workflows and do not have established modelling capabilities.

Beta-hydroxybutyrate and the Forensic Pediatric Autopsy: A Retrospective Case Series

A Lafrenière¹, C Milroy², J Parai²

¹Texas Children's Hospital, Baylor College of Medicine, Houston, Texas; ²The Ottawa Hospital, The Eastern Ontario Regional Forensic Pathology Unit, Ottawa, Ontario

Background: Beta-hydroxybutyrate (BHB) is used both clinically and in the autopsy setting as a marker for diabetic and alcoholic ketoacidosis in addition to other causes of ketoacidosis. In the adult, post-mortem BHB concentrations in non-ketoacidotic deaths ranges from 0.05 – 2.44 mmol/L. Adult BHB values for the post-mortem diagnosis of ketoacidosis vary, with published threshold fatal values ranging from 1 mmol/L upwards. Post-mortem values for the diagnosis of ketoacidosis have not been assessed in the pediatric population.

Methods: The records of the Forensic Pathology Unit were searched for pediatric deaths (decedent less than 18 years of age) with elevated levels of vitreous (>2 mmol/L) or blood (>200 mg/L) BHB between January 1, 2010 to December 31, 2020. Autopsy reports were reviewed to obtain demographic information, clinical symptoms, post-mortem biochemistry, and pathology. Histology of the heart, lung, liver, and kidneys were reviewed by two authors blinded to the autopsy information. Statistical analyses were performed to compare histological changes with BHB levels and to assess for any associations between the histologic features.

Results: 400 pediatric autopsies were performed during the study period, of which 16 met the inclusion criteria. The mean age was 7.03 years with a median age of 4.5 years. The cause of death was attributed to diabetic ketoacidosis in two cases, one of which was related to maternal diabetic ketoacidosis in a case of intrauterine death. Other causes included infections (n=5), trauma (n=2), congenital heart disease (n=2), unascertained (n=3), malignancy, and mixed drug toxicity. The mean concentration of vitreous BHB was 3.56 mmol/L (median 2.52 mmol/L; n=13 cases) and blood BHB demonstrated a range from <50 mg/L to 1188 mg/L (n=8 cases). Clinically, 69% of children with elevated BHB had reported multiple days of symptomatology, including fever, myalgia, or diarrhea; in one case lacking these symptoms, there was evidence of infection within the lung, indicative of a prolonged period of illness. Cases with severe hepatic steatosis and renal subnuclear vacuolation each had BHB concentrations that were higher than those with no, mild, and moderate changes (p=0.019). Diffuse hepatic nuclear glycogenation was associated with cases demonstrating renal subnuclear vacuolation (p=0.0027).

Conclusion: Elevated BHB was identified in blood and vitreous in fatal non-diabetic cases, including infection and malignancy. Histological changes were associated with elevated BHB levels. Diabetic ketoacidosis was associated with the highest level of BHB; however, over half of the cases studied demonstrated a vitreous BHB greater than 2.5 mmol/L. Further evaluation of a fatal BHB threshold for the pediatric population should be considered.

Spectrum of Autopsy Findings in COVID-19 Related Pediatric and Fetal Deaths: 4 Cases from a Tertiary Care Children's Center

F Malik, J Kasten, K VandenHeuvel, D Leino, A Bernieh

Cincinnati Children's Hospital Medical Center, Cincinnati, Ohio

Background: Although Coronavirus disease 19 (COVID-19)-associated mortality is correlated with age and specific pre-existing morbidities, pediatric infection is common, represents an increasing percentage of overall incident infection, is occasionally lethal, and may be rarely associated with the delayed and potentially critical Multisystem Inflammatory Syndrome in Children (MIS-C). The virus crosses the placenta in infected pregnant women, causing placental complications and intrauterine fetal demise (IUFD). We examine the cross-sectional spectrum of pediatric COVID-19 autopsy pathology.

Methods: All post-mortem examinations of deaths due to maternal or pediatric antemortem COVID-19 infection performed at a tertiary children's hospital from June 2020 to August 2021 were reviewed.

Results: Two cases each of fetal and pediatric deaths were reviewed. In all cases, COVID-19 infection was confirmed either by serology or polymerase chain reaction (PCR) testing. Examination of each pediatric case was restricted to body only and brain only. **IUFDs:** The anatomically normal fetuses died at 24 and 36 weeks gestation, respectively. The cause of death in both was placental insufficiency secondary to massive perivillous fibrin deposition, and chronic histiocytic intervillitis with trophoblast necrosis. COVID-19 was confirmed by IHC (2/2) and PCR (1/2) on formalin fixed paraffin embedded placental and fetal liver tissue. Both mothers presented with mild symptoms. **Childhood Deaths:** The pediatric deaths were in females aged 9 years and 19 years, respectively. Recent COVID-19 infection was confirmed by serology. Brain exam in the 9-year-old showed massive, multiple infarct-like parenchymal necrosis, hemorrhage, cystic cavitation, and perivascular lymphohistiocytic infiltrate without thrombi or flow abnormalities. Additional testing did not reveal other causes. The 19-year-old had Ebstein anomaly, 13 years status post orthotopic heart transplant with high-grade acute cellular rejection. Death was caused by cardiac tamponade and multi-organ failure due to pulmonary artery origin massive hemomediastinum (1000 ml), attributed to COVID-19 related MIS-C causing coagulopathy. Acute vasculitis and prominent endothelial cells rendered histologic support for recent COVID infection.

Conclusion: We present autopsy findings in 4 cases of pediatric and fetal deaths due to recent COVID-19 infection. Observed placental lesions leading to insufficiency and IUFD are consistent with previously published reports. The CNS findings of hypoxic-ischemic encephalopathy are attributed to the direct viral damage, previously documented in adults. To the best of our knowledge, this series highlights the first pediatric autopsy findings in a cardiac transplant recipient succumbing to sequelae of COVID-19 related MIS-C.

PLATFORM III: Neoplasia

17

Hepatocellular malignant neoplasm, NOS exhibits distinct and more complex copy number alterations than conventional hepatoblastoma

S Zhou, D Estrine, D Ostrow, M warren, N Shillingford, L Wang, R Schmidt, G Raca, L Mascarenhas, J Biegel, J Ji

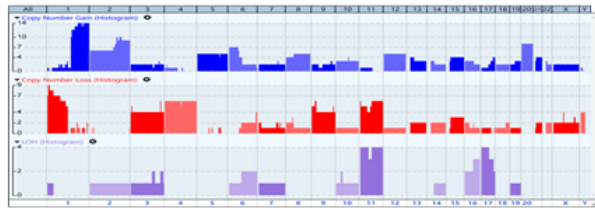
Children's Hospital Los Angeles, Los Angeles, California

Background: Hepatocellular malignant neoplasm, not otherwise specified (HCN-NOS) is a rare and poorly understood primary liver cancer with overlapping histology features of conventional hepatoblastoma (HB); thus, it is often diagnostically challenging to distinguish HCN-NOS from HB. As a major source of genomic variations driving tumor initiation and evolution, DNA copy number variants (CNVs) have been associated with numerous tumor types. Detection of recurrent CNVs may provide diagnostic as well as prognostic biomarkers to assist clinical diagnosis and management. So far, it is unknown whether HCN-NOS and HB show different CNV profiles.

Methods: Chromosomal microarray analysis using OncoScan/Cytoscan HD (Thermo Fisher Scientific) was performed on a total of 13 primary tumors and one recurrent tumor from 13 HCN-NOS patients, and 20 primary tumors and one recurrent tumor from 20 HB patients. Copy number profiles were compared between the two groups.

Results: CNVs were detected in 14/14 HCN-NOS specimens (Figure A). In contrast, 18 of 21 HB specimens had CNVs and there were more gains than losses (Figure B). HCN-NOS showed the following recurrent CNVs with an overall frequency higher than 20%: gain of 1q (100%), 2q (64.3%), 20 (57.1%), 6p (50%), 2p (42.9%), 5 (35.7%), 8 (35.7%), 12 (35.7%), 15 (28.6%), 17q (28.6%), 21 (28.6%), and 10 (21.4%); loss of 1p (50%), 4 (42.9%), 11q (42.9%), 9p (35.7%), 11p (35.7%), 3 (28.6%), 9q (28.6%), Y (28.6%), and 15 (21.4%); and copy neutral loss of heterozygosity (CN-LOH) in chromosome 11 (28.6%) and 17p (28.6%). For HBs, there were recurrent gains of 1q (52.4%), 2q (47.6%), 20 (42.8%), 2p (38.1%), 8 (33.3%), 6 (23.8%), 12 (23.8%), 17 (23.8%), 7 (19.0%), and 5 (14.3%); recurrent losses of 4q (19.0%) and 1p (9.5%); and CN-LOH of 11p15.5 (33.3%). Gain of 1q ($p = 0.002$), losses of 3 ($p = 0.019$), 4p ($p = 0.002$), 9 ($p = 0.019$), 11p ($p = 0.006$), 11q ($p = 0.002$) and Y ($p = 0.019$), and CN-LOH in 17p ($p = 0.019$) were more frequently observed in HCN-NOS group compared to the HB group. There were no significant differences in gains of 2q ($p = 0.491$) and 20 ($p = 0.5$), loss of 4q ($p = 0.151$), or CN-LOH of 11p15.5 ($p = 1.0$) between the two groups. The recurrent HCN-NOS tumor showed additional CNVs compared to the primary tumor. For the HB case with both primary and recurrent tumors, there were no clinically significant CNVs identified in either tumor. No high-level gene amplification events were found in any

tumor.



A. Summary of copy number variants (in numbers) in HCN-NOS



B. Summary of copy number variants (in numbers) in HB

Conclusion: HCN-NOS showed frequent and more complex CNVs than HB. Chromosome 1q gain was predominant in both groups but appeared to be more common in the HCN-NOS group. Loss of chromosomes 3, 9 and Y, as well as CN-LOH in 17p were seen exclusively in the HCN-NOS group.

Clinicopathologic study of hepatic adenomas: A Children's Hospital Experience.

Y Estrella, N Cortes-Santiago, M Blessing, K Patel

Texas Children's Hospital, Houston, Texas

Background: To study clinicopathologic features of hepatic adenomas in children; including background liver, and identify differences, if any, from adult population.

Methods: Pathology database was queried to identify all cases of hepatic adenomas from 2003 to 2021. Medical records and archived pathology material was reviewed in a retrospective manner.

Results: Of the 22 patients identified, 12 were females with median age at diagnosis 12 years (1.5 to 21 yrs). Background liver showed: cirrhosis (6), steatosis (4), NRH (1), hepatoblastoma (2), sickle cell disease (3), post chemotherapy for hepatic angiosarcoma (1), and normal (4). Cirrhosis was secondary to congenital hepatic fibrosis (1), cryptogenic (1), biliary atresia (1), alpha1-anti trypsin deficiency (1), FXR deficiency (1), and sclerosing cholangitis (1). Hepatic steatosis with or without obesity was limited to females. History of prednisone was noted in 8 patients (5F:3M) and oral contraceptive pills in 2 females of whom 1 was transitioning to male with subsequent exposure to androgens. Ten patients had multiple lesions on imaging of whom 5 underwent transplantation, 1 right hepatectomy and 4 are under observation with or without growth in mass. Six out of 8 patients with a solitary lesion underwent partial resection, 1 transplantation and 1 is under follow up. Four patients had no mass on imaging and adenoma was diagnosed incidentally in 3 from the cirrhotic explanted liver. Vast majority (16/22, 72.7%) of adenomas were composed of large, pale, vacuolated and variably steatotic hepatocytes with loss of LFABP expression in 7 out of 9 cases studied and HNF1alpha mutation in 2 out of 4 cases tested. Of the 6 non-steatotic lesions, peliosis was a dominant feature in 4 (2 showing dilated sinusoids engorged with sickled cells), and cholestasis in 2. Lesional inflammation was predominantly lymphocytic, mild and limited to the stroma around the unpaired vessels. All were negative for glutamine synthetase and GPC-3 expression. Only one adenoma occurring in a FAP patient had nuclear reactivity for beta catenin, the rest were membranous. CD34 was largely perivascular (86.6%) and rarely diffuse (13.3%). None showed significant cytologic atypia. Three patients were lost to follow up, one was deceased (graft dysfunction); none showed recurrence of adenoma.

Conclusion: In contrast to adults, vast majority of pediatric hepatic adenomas occur in cirrhotic or abnormal livers (~82%). Outside of cirrhosis, hepatic steatosis seems to be a predisposing factor in females. Adenomas were frequently steatotic with loss of LFABP expression that did not necessarily correlate with HNF1alpha mutation on few samples that were tested. Long term clinical outcome is dependent on patients' underlying medical condition with no recurrence of adenoma in our series.

Histologic Characterization of Pediatric Mesenchymal Neoplasms with Kinase Alterations Treated with Targeted Therapy

E Baranov¹, J Davis², K Winsnes², M Breen¹, K Janeway³, S DuBois³, A Church¹, A Al-ibraheemi¹

¹Boston Children's Hospital, Nahant; ²Oregon Health & Science University, Portland, Oregon; ³Dana-Farber/Boston Children's Cancer and Blood Disorders Center, Boston, Massachusetts

Background: Recurrent alterations involving receptor tyrosine or cytoplasmic kinase genes have been described in soft tissue neoplasms such as infantile fibrosarcoma (IFS) and inflammatory myofibroblastic tumors (IMT). Recent trials and regulatory approvals for targeted inhibitors against the kinase domains of these oncoproteins have allowed for increased use of targeted therapies in these patients. We aim to characterize the histologic features of pediatric mesenchymal neoplasms with kinase alterations treated by targeted inhibition.

Methods: Eight children with tyrosine kinase-altered mesenchymal neoplasms with pre- and post-treatment material were identified. Clinical, radiologic, and molecular information was collected and a detailed histologic review was performed

Results: Tumors occurred in 5 females and 3 males with a median age at presentation of 6.5 years (range 0-15 years). Median radiologic tumor size at presentation was 7.5 cm (range 4.2 – 15.7 cm). Tumor sites included somatic soft tissue (n=5) and viscera (n=3). Pre-treatment diagnoses were: IMT (n=3), epithelioid inflammatory myofibroblastic sarcoma (n=1), and descriptive diagnoses (n=4) such as “kinase-driven spindle cell tumor”. Fusions identified were *ETV6-NTRK3* (n=2), *TPM3-NTRK1*, *SEPT7-BRAF*, *TFG-ROS1*, *KLC1-ALK*, *RANBP2-ALK*, and *MAP4-RAF1*. Patients were treated with larotrectinib (n=3), ALK inhibitors (n=3), and MEK inhibitors (n=2) prior to resection/biopsy. Duration of treatment prior to biopsy/resection ranged from 5-24 months (median 9 months). Pre-treated tumors were moderately to markedly cellular, and composed of spindled to plump ovoid cells in a variably myxoid to collagenous stroma. Inflammation was marked in half of cases. In contrast, post-treatment tumors exhibited marked decrease in cellularity (7/8), collagenous stroma (7/8) with extensive glassy hyalinization (5/8). Necrosis and mitoses were largely absent (7/8). In 2 cases, abundant coarse or psammomatous calcifications were seen and in one case prominent perivascular hyalinization was noted. Inflammation was typically sparse. Residual viable tumor was seen in 3/8 cases (<5% in one case, and >75% in 2/8 cases)

Conclusion: Mesenchymal neoplasms with tyrosine kinase alterations treated with kinase inhibitors show a constellation of histologic features markedly different from the original pre-treatment tumors. These features include significantly decreased cellularity, collagenous or fibrous stroma (often with extensive glassy hyalinization), absent mitotic figures, occasionally prominent stromal calcifications and sparse to moderate lymphoplasmacytic inflammation. Presence of these histologic features may be helpful in assessing tumor response after treatment with kinase inhibitors

FGFR1-rearrangements in pediatric spindle cell tumors

A Al-Ibraheemi¹, L Wang², D Parham², C Beadling³, C Lockwood⁴, E Rudzinski⁵, J Davis³

¹Boston Children's Hospital, Boston, Massachusetts; ²Children's Hospital Los Angeles, Los Angeles, California; ³Oregon Health & Science University, Portland, Oregon; ⁴University of Washington Medical Center, Seattle, Washington; ⁵Seattle Children's Hospital, Seattle, Washington

Background: Recurrent genetic alterations in kinases within the MAP kinase pathway are described in infantile fibrosarcoma (IFS)/cellular congenital mesoblastic nephroma (cCMN) and the group of spindle cell tumors provisionally designated “*NTRK*-rearranged” spindle cell tumors. These tumors demonstrate overlapping morphologies, immunophenotype, and spectrum of kinase alterations including in *NTRK1/2/3*, *RET*, *MET*, *ABL1*, *ALK*, *RAF1*, and *BRAF*. The relationship between IFS/cCMN and the provisional entity is not fully elucidated. To-date, one case in an adult patient with a uterine fibrosarcoma-like tumor (placed in the category of “*NTRK* rearranged” spindle cell tumor) has been reported to harbor an activating *FGFR1* gene fusion. Herein we describe 2 pediatric patients with IFS-like tumors, both harboring *FGFR1* gene fusions.

Methods: Two *FGFR1*-rearranged pediatric mesenchymal neoplasms were identified; 1 as part of a prior research study on *NTRK* tumors and 1 through routine clinical practice. Clinicopathologic features were assessed. Both underwent partner agnostic targeted NGS on clinically validated platforms.

Results: Patient 1 was an infant female who presented at 3 months with a 4.2 cm perirectal soft tissue tumor. The tumor was biopsied and then resected via proctectomy. The diagnosis was that of a low-grade spindle cell neoplasm, with a variant of infantile fibrosarcoma favored. The resection had negative margins and no further therapy was pursued. At 5 years of follow-up, the patient was alive with no evidence of disease. As part of a separate study, NGS was performed showing a *FGFR1-PARD68* fusion. Patient 2 was an infant male who presented at 9 months with a 7.5 cm intrapelvic to thigh soft tissue tumor. The tumor was biopsied and diagnosed as spindle and round cell neoplasm with *FGFR1-EBF2* gene fusion. The patient was started on lenvatinib therapy (multi-tyrosine kinase inhibitor with activity against FGFR1). The patient is now 3 months into therapy with stable disease. Morphology of both cases were similar, including intratumoral heterogeneity, variable cellularity with spindled to ovoid cells embedded in a spectrum of minimal to robust collagenized stroma and focal areas of myxoid change. Both showed strong, patchy staining of CD34; no expression of S100 or other immunomarkers was present.

Conclusion: We present the first series of *FGFR1*-rearrangements in IFS-like pediatric tumors, including a patient treated with lenvatinib therapy. Our series expands the spectrum of kinase drivers within IFS-like tumors and reinforces the compelling overlap between IFS/cCMN-like tumors and the provisional entity of “*NTRK*-rearranged spindle cell tumors.” Knowledge of potential genetic alterations in this spectrum of tumors is a key for diagnostic and targeted therapeutic purposes.

Spatial Gene Expression in Childhood Ependymoma Reveals Tumor Cell Subpopulations and Their Locations In Situ

N Willard¹, A Griesinger², R Fu², K Riemondy², J Hesselberth², G Norris¹, V Amani², F Harris², E Grimaldo², N Foreman¹, A Danson¹

¹Children's Hospital Colorado, Aurora, Colorado; ²University of Colorado, Aurora, Colorado

Background: Ependymoma (EPN) is an aggressive childhood CNS tumor with high recurrence rates. Posterior fossa (PF) EPN is divided into two molecular subgroups, Group A (PFA) and Group B (PFB). PFA, particularly relapsed PFA, is fatal with limited treatment options. Thus, there is a need to better understand PFA biology. While single cell RNA sequencing (scRNAseq) has defined tumor cell subpopulations within PFA EPN, it does not provide any architectural expression data. Though immunohistochemistry (IHC) can help, it is a piecemeal approach. Here, we use spatial transcriptomics to overcome this.

Methods: Frozen tissue from 10 PFA EPN was embedded, sectioned, and permeabilized on a Visium slide (10x Genomics) containing 5000 RNA capture spots. Barcoded libraries were generated for each spot and sequenced (Illumina HiSeq6000). Data was deconvoluted, aligned to the genome, and analyzed to identify clusters of transcriptionally-related spots. Expression data was superimposed onto H&E using Loupe Browser. Analysis packages were applied to detect lineage trajectories (Slingshot) and cell-cell crosstalk based on ligand-receptor pair expression (CellChatDB).

Results: Mapping of transcripts to PFA histology robustly detects tumor subpopulations identified by scRNAseq. Tumors consist largely of transportive cells (TEC), ciliated cells (CEC) restricted to rosettes, and mesenchymal cells (MEC) in perinecrotic zones. Further localization was observed, such as ciliation, a function of differentiation, being a feature of hypocellular regions. Because this technique allows analysis of gene expression at a light microscopy level, we examined mitotic genes in subpopulations, revealing that mitotically active cells were restricted to the TEC subpopulation. This novel finding impacts our understanding of the lineage trajectory and identifies potentially relevant tumor progenitors. To this end we have refined lineage trajectories to include the physical proximity of cells, showing concordance of trajectories with transitioning of cell types across the tumor from areas of TEC to CEC and MEC cells. These data can also be used to refine ligand-receptor pair analyses by factoring in the proximity of ligand-receptor pairs, and was used to identify discrete cell-cell signaling pathways in TEC and MEC zones.

Conclusion: This transformative technology enables gene expression analysis at a histologic level. We can map subpopulations identified by scRNAseq to tumor architecture more definitively and rapidly than IHC. We demonstrate that bioinformatic approaches to detect cell lineage trajectories and cellular crosstalk in scRNAseq can be refined with spatial transcriptomic data. These novel insights advance our understanding of PFA EPN, a critical step in improving treatment options for children with this disease.

Comprehensive genomic profiling of pediatric leukemia: a single institution's experience

K Chisholm¹, K Tsuchiya²

¹Seattle Children's Hospital, Seattle, Washington; ²University of Washington, Seattle, Washington

Background: Many recent discoveries have been made in the molecular landscape of leukemias, especially in pediatric leukemias. Identification of chimeric fusion transcripts by RNA analysis and mutations by next-generation sequencing can aid in prognostication, guide potential therapies, and provide minimal residual disease screening strategies. However, it remains unclear if all cases, or only a subset, warrant such testing at diagnosis.

Methods: With a predetermined algorithm, the majority of new and relapsed diagnoses of acute myeloid leukemia (AML), mixed phenotype acute leukemia (MPAL), B-lymphoblastic leukemia/lymphoma (B-ALL), T-cell lymphoblastic leukemia (T-ALL), and early T-cell precursor ALL (ETP-ALL) underwent DNA and RNA testing in addition to the conventional diagnostic karyotype and fluorescence in situ hybridization (FISH). DNA testing included a chromosomal SNP microarray (CMA) and next generation DNA sequencing (NGS) using a panel of 340 genes to detect structural variants, single nucleotide variant (SNVs), insertion/deletions, and copy number variants. RNA NGS was performed on an Archer custom FusionPlex panel with ~50 gene targets.

Results: Over a period of 15 months, 80 new or relapsed diagnoses of leukemia/lymphoblastic lymphoma were made. In the 10 tested AML/myelodysplastic syndrome (MDS)/MPAL, 4 had relevant SNVs (*FLT3* tyrosine kinase domain, *KIT*, *WT1+FLT3* internal tandem duplication), one had *BRCA1* mutation confirmed to be germline, 3 had *KMT2A* fusion partners clarified, and 1 had a cryptic *NUP98-NSD1* fusion identified. In the 34 tested B-ALL, CMA identified important copy number alterations and deletions (such as *IKZF1*, *ERG*, *CREBBP* and *P2RY8-CRLF2*) in 9 patients. DNA testing confirmed the same deletions, and additionally identified 1 case with relevant therapy-related SNV (*JAK2*), and 7 cases with potential germline predisposition pathogenic mutations (most confirmed somatic on follow-up). RNA testing identified a cryptic *BCR-ABL1* fusion in 1 case which influenced prognosis and an *IGH-BCL6* fusion in a triple hit lymphoma/leukemia. In the 12 T-ALL/ETP-ALL, the significant findings were potential germline predisposition pathogenic variants identified in 4 cases, including *ATM* (already known in a sibling) and *NF1*.

Conclusion: Based on these findings, we have further refined our DNA and RNA testing algorithm to better balance detection of clinically significant genomic alterations with cost-effectiveness. This algorithm includes DNA NGS and RNA on all AML/MPAL. For B-ALL, we recommend CMA in all cases, DNA NGS in Ph-like and hypodiploid, and RNA in Ph-like cases or those with normal FISH. For all other cases, we would only recommend DNA testing of the leukemia if it were paired with a germline specimen to exclude any germline pathogenic variants.

Well-Differentiated Neuroendocrine Tumors of the Appendix in Children, Clinicopathologic Study

C Simon, P Ehrlich, L Sedig, A Hryhorczuk, T Stoll, R Rabah, A Heider

University of Michigan, Ann Arbor, Michigan

Background: Neuroendocrine tumors (NET) of the GI are rare, however, they are the most common epithelial tumor of the GI tract in children. Well-differentiated appendiceal NET are typically incidental. NET rarely cause symptoms or secrete hormones. There are currently no diagnostic studies specific for NET and minimal consensus regarding imaging findings. Few studies of NET have been done in the pediatric population and practice guidelines for management of appendiceal NET are mainly based on adult data. Our study aims to identify clinical, radiological, and pathological findings in pediatric NET, test criteria for treatment, review potential prognostic pathological findings and possible diagnostic radiological studies.

Methods: A retrospective data search was conducted for well-differentiated NET of the appendix in patients ≤ 21 years between 1/1/03-7/1/21. Available clinical, radiologic, pathological, and follow-up information was recorded.

Results: 32 patients with NET in the pediatric population were identified. No masses were reported in the patients who underwent presurgical imaging. Review of the appendectomy showed NET (0.2-4 cm) most commonly located in the tip of the appendix, when specified. The vast majority of cases were WHO G1 (29/32). The majority of tumors extended to the subserosa/ mesoappendix (13) with negative margins (21/32). Lymphovascular (5), perineural (1) and both lymphovascular and perineural invasion was noted (2). The specified tumor stages were pT1 (7), pT3 (13), pT4 (5). Patients who underwent laboratory testing for chromogranin A (15) and urine 5H1AA (13) were within normal limits. Surgical resection was performed in 9/10 recommended cases. The indications for surgery were size (1), location (1), mesoappendix involvement (1), size and margin involvement (2), LVI and size (2), LVI (1) and unclear (1). 8 subsequent resection specimens were available for review. No residual disease was noted. 4/8 cases noted lymph node metastasis. No patients who had follow-up radiology had evidence of metastatic disease. In patients where clinical follow-up is available no evidence of disease is noted.

Conclusion: Our study showed that all well-differentiated appendiceal NET were incidentally found as part of acute appendicitis workup/management. The vast majority of NET were localized with low-grade histology. Our small cohort support the previously suggested management guidelines. Our radiologic review didn't identify a best modality for NET. Comparing cases with and without metastatic disease, no tumors under 1 cm had metastasis, but grade, extension and lymphovascular invasion alone do not correlate with presence of metastasis. To date, all our patients have no recurrent or additional metastatic disease.

Is Splenic Lymphatic Malformation with Papillary Endothelial Proliferation a Unique Entity or a Morphologic Variant?

J Slack¹, J Putra², M Callahan¹, W Eng³, L Teot¹, A Church¹, A Perez-Atayde¹

¹Boston Children's Hospital/Harvard University, Boston, Massachusetts; ²University of Toronto/Hospital for Sick Children (SickKids), Toronto, Ontario; ³Dana Farber Cancer Institute/Boston Children's Hospital/Harvard University, Boston, Massachusetts

Background: Lymphatic malformations (LM), also known as lymphangiomas, are congenital anomalies due to abnormal development of the lymphovascular system. They are often multifocal, affect many organ systems, and are associated with a number of developmental or overgrowth syndromes. Splenic LMs are rare and usually occur in the context of multi-organ disease. Isolated LM confined to the spleen, are even rarer, and a subset of these may show unique papillary endothelial proliferations that may mimic malignancy. It is unknown if these represent a distinctive entity or an unusual variant of lymphatic malformation. To the best of our knowledge, only 7 cases have been reported previously.

Methods: We present an additional 3 cases of splenic LM with papillary endothelial proliferation, summarizing their clinical, radiological, pathological, electron microscopical and molecular findings.

Results: Case 1 was a previously healthy 16-year-old girl who presented with two-week history of abdominal pain and nausea. Case 2 was an 8-year-old girl with a medical history and genetic work-up suggestive of Dravet syndrome who had a splenic mass incidentally noted on ultrasonography to screen for kidney stones. Case 3 was a 2-year-old girl with PIK3CA-related overgrowth syndrome, who despite normal splenic imaging several months prior, had a new splenic mass incidentally noted on routine imaging studies for clinical trial inclusion. Radiologically, each of the 3 children had an isolated splenic solid mass with central radial scar, which imparted a characteristic 'spoke-and-wheel' appearance. Histologically, the lesions consisted of lymphatic channels with unusual papillary endothelial proliferations. Electron microscopy and immunohistochemical studies confirmed a lymphatic nature of the endothelium. Molecular testing was negative in Cases 1 and 2, while in Case 3 a PIK3CA mutation (c.3139C>T; 19% of 153 reads) was identified.

Conclusion: We report 3 cases of splenic LM with papillary endothelial proliferation in a pediatric cohort. It is important to recognize this rare entity as it can mimic malignancy. Although occurring in 3 different clinical contexts, all lesions had similar histopathology and shared a characteristic radiologic appearance. Molecular testing was intriguing, with the first 2 cases being negative, while in the third case no additional mutations, aside from a previously known somatic PIK3CA mutation, were identified. As such, it remains unknown if this represents a unique organ-specific vascular anomaly, or is simply an unusual morphologic variant of a lymphatic malformation that occurs in the spleen. A team-based approach that incorporates clinical, radiological, pathological, and molecular findings is key, and in our series, enabled early diagnosis that allowed 2 children to avoid splenectomy.

POSTERS

25

The Natural History of 17 α -Hydroxylase Deficiency Illustrated by Two Gonadectomy Cases

E Ferreira¹, M Curtis¹, P Frosk², J Gingerich³, M Rosenthal⁴, A Morris⁴, C Stefanovici¹

¹Department of Pathology, University of Manitoba, Winnipeg, Manitoba; ²Department of Biochemistry and Medical Genetics, Winnipeg, Manitoba; ³Section of Hematology/Oncology, Department of Internal Medicine, Winnipeg, Manitoba; ⁴Department of Obstetrics, Gynecology & Reproductive Sciences, Winnipeg, Manitoba

Background: 17 α -hydroxylase-deficiency is an autosomal recessive disorder of steroid synthesis resulting in mineralocorticoid excess and underproduction of glucocorticoids and sex hormones. In 1989, several individuals from a local Mennonite community were identified with 17 α -hydroxylase/17,20-lyase deficiency due to a frameshift founder mutation (CYP17A1:c.1435_1438dup).

Methods: We present two individuals (16&45-years-old) with female phenotype and XY-karyotype who presented in their teens 27-years apart with hypertension, amenorrhea, and undetectable cortisol. The first patient initially declined gonadectomy and tried to hide her disease through adulthood including when presenting for medical care. Twenty-five years later, she presented with multiple bulky retroperitoneal masses and lymphadenopathy whereupon extensive resection was performed. Two years later, the second patient (16-years-old) was diagnosed with 17 α -hydroxylase-deficiency and advised to undergo prophylactic gonadectomy. Although not direct relatives, the teenager was convinced undergo early gonadectomy by the first patient.

Results: The 45-year-old was diagnosed with extensive poorly-differentiated germ cell tumor and metastatic adenopathy. Prior to resection, she had not shared her history of 17 α -hydroxylase-deficiency. However, with further questioning following pathologic diagnosis, she revealed her previous diagnosis and underwent adjuvant chemotherapy. The 16-year-old underwent bilateral gonadectomy showing hypogonadism and cryptorchidism with abundant Sertoli cells, Leydig cell paucity and an ectopic adrenal gland focus. There was no intratubular-germ-cell-neoplasia.

Conclusion: These cases confirm necessity of timely prophylactic gonadectomy. Additionally, they demonstrate the importance of thorough family history especially in the context of a sensitive or rare condition. Most importantly, the cases underscore the importance of accessible supports for patients with disorders of sexual differentiation.

Series of Undifferentiated Round Cell Sarcomas with Unique Molecular Aberrations

J Gulliver, A Richardson, P Chou

Lurie Children's Hospital, Chicago, Illinois

Background: Undifferentiated round cell sarcomas are aggressive tumors comprised of small round blue cells. To date, many tumors in this category have not shown a consistent identifiable underlying molecular abnormality. We report two cases of undifferentiated round cell sarcomas with unique molecular aberrations.

Methods: Clinical information was obtained from patient records. In the first case, an 8 year old female presented with intermittent left leg pain. Imaging showed an 8.6 cm mass lesion centered in the left proximal metadiaphyseal region of the left tibia causing cortical destruction and marrow replacement with a periosteal reaction and associated soft tissue component. In addition, metastases to the liver, pancreas, breast, and cranium were also identified. In the second case, a 13 year old female presented with cough and chest pain. Imaging showed a large mediastinal mass as well as metastatic disease to the liver, thoracic and lumbar spine.

Results: In the first case, biopsy of the left tibia lesion revealed sheets of small round blue cells with scant cytoplasm, frequent apoptosis, and extensive necrosis. The tumor was positive for synaptophysin. CD99 showed focal patchy membranous positivity. SATB2 showed patchy nuclear positivity. INI1 (BAF47) was retained. CAM5.2, AE1/AE3, Chromogranin, Desmin, Myogenin, MYOD1, PHOX2B, BCOR, WT-1 (n-terminus), WT-1 (c-terminus), S100, SOX10, and CD61 were negative in the lesional cells. Variants of potential clinical significance were identified in RB1 gene on chromosome 13. Potential copy number variations on chromosomes 1q, 2p, and 6q were also identified. In the second case, biopsy from the brain revealed undifferentiated ovoid cells with scattered necrosis and brisk mitotic activity. The tumor was positive for CD56 and FLI-1. The tumor was negative for CD99, Synaptophysin, CD34, WT1 (n-terminus), WT1 (c-terminus), AE1/AE3, EMA, Myogenin, Desmin, Tyrosine hydroxylase, PAX8, PAS, PAS-D, CD1a, CD99, Synaptophysin, S-100, CD3, CD20, CD45, and TdT. A heterologous deletion of CDKN2A on chromosome 9 was identified.

Conclusion: Pediatric undifferentiated round cell sarcomas are rare aggressive malignancies. Rb1 alterations have been identified in tumors with increased anaplasia and pleomorphism. In addition, abnormalities involving CDKN2A have been associated with a poor prognosis. While fusion patterns are beginning to emerge, there is still a subset of tumors with novel molecular abnormalities. Characterization of these tumors will be important for diagnosis and future therapeutic targets.

Multi-organ Involvement of Epithelioid Hemangioendothelioma: An Unusual Case

C Le Phong, M Takeda, R Mahabir, S Zhou, N Shillingford, M Warren, W Huh, R Schmidt, J Miller, S Durham B Pawel, L Wang

Children's Hospital of Los Angeles, Los Angeles, California

Background: Epithelioid hemangioendothelioma (EHE) is a rare, malignant endothelial neoplasm. Although EHE can arise throughout the body, the most common sites of involvement include liver, lung, and bone. EHE usually occurs in adults, rarely in children, and may arise as a solitary lesion or with multifocal involvement. Two genetic subtypes are currently well-defined including *WWTR1-CAMTA1* and *YAP1-TFE3*. We present an unusual case of EHE with multi-organ involvement in a teenage boy.

Methods: A 17-year-old previously healthy male complained of mild, intermittent neck pain 7 months ago. An IR-guided biopsy of the cervical spine performed in Mexico 3 months ago was suggestive of a schwannoma. One month ago, CT and MRI at CHLA demonstrated a lytic expansile C1 mass lesion (6.1 cm), innumerable liver lesions (up to 14.3 cm), few small lung nodules, and small bony nodules in the skull and spine. Initial C1 and liver biopsies were inconclusive. Repeat open biopsy of the C1 mass was then performed.

Results: The first C1 mass core biopsy was non-diagnostic due to scant tissue. The core biopsy of the liver mass showed few scattered large cells that expressed CD31, CD34, and CD61, favoring megakaryocytes. No definitive mass was identified. The open biopsy of the C1 mass showed small and large polygonal cells with abundant eosinophilic cytoplasm, scattered large multinucleate forms with prominent eosinophilic intranuclear pseudo-inclusions, and rare endothelioid spaces containing fragmented RBC-like inclusions. Rare mitotic figures were noted. The lesional cells expressed CD21, SATB2, CD61, ERG, CD31, Factor VIII, CAMTA1, TFE3 (variable), CAM5.2 (focal), and CD68 (variable). RNA sequencing studies revealed a *WWTR1-CAMTA1* fusion, confirming the diagnosis of EHE. Retrospective analysis of the liver biopsy revealed rare eosinophilic intranuclear pseudo-inclusions within the large cells, which also expressed FLI1, TFE3 (partial), Factor VIII, and CAMTA1, consistent with EHE.

Conclusion: This case illustrates the diagnostic difficulty in diagnosing EHE and other vascular lesions in small biopsies with only rare lesional cells present. The finding of megakaryocyte-like cells in liver tissue, though present in a number of benign conditions, should prompt the possibility of the presence of the neoplastic cells of EHE in the setting of multiple mass lesions in various organs. If needle biopsy material is insufficient for diagnosis, repeat larger biopsies allow for more readily identifiable classic and typical features of EHE. Immunostaining with CAMTA1 and/or TFE3 will be of great help in the differential diagnosis and further molecular studies can confirm the diagnosis.

Role of Intrapulmonary Bronchopulmonary Anastomoses in Severe COVID-19-related Hypoxemic Acute Respiratory Failure

J Bodmer¹, A Levin¹, C Westöö², O Van Der Have², K Tran Lundmark², S Abman¹, C Galambos¹

¹Children's Hospital Colorado, Aurora, Colorado; ²Lund University, Lund

Background: Mechanisms contributing to the often “silent” but severe hypoxemia leading to acute respiratory failure (ARF) experienced by many SARS-CoV2 infected patients are poorly understood. Although pulmonary histopathology including hyaline membrane disease, small vessel thrombi and endotheliitis are well-documented, the microscopic basis for profound hypoxemia in COVID-related ARF is yet to be fully characterized. Recent radiologic, transcranial bubble ultrasound and three-dimensional (3D) histologic image reconstruction studies show the presence of right-to-left intrapulmonary shunt that is potentially due to the recruitment of intrapulmonary bronchopulmonary anastomoses (IBAs). IBAs are considered unique, right-to-left vascular shunts that utilize the bronchial circulation to direct blood from the pulmonary arteries to pulmonary veins while bypassing alveolar capillaries. We report an autopsy case of a 17-year-old female with obesity who died of COVID-related ARF shortly after an acute onset of shortness of breath, dyspnea, and chest pain. We extensively studied her lungs after death using state-of-the-art imaging methods to determine the presence of IBA recruitment in COVID-related ARF.

Methods: Following autopsy evisceration, the main pulmonary vessels were cannulated and injected with tissue ink and 20 tissue blocks were prepared for extensive studies. Routine H&E stains with serial sections of selected blocks were performed, and immunohistochemical staining for smooth muscle actin and the endothelial marker, CD31, was performed. The pathways of IBAs were further studied by microCT and synchrotron-based phase-contrast imaging followed by 3D image reconstruction.

Results: At autopsy, the lungs were consolidated and heavy. Evolving hyaline membrane disease, extensive acute and focally-organizing thrombi within small, medium, and large sized pulmonary arteries dominated the histology. Additional findings included occasional bronchiolar fibrin casts/plugs, patchy hemorrhagic necrosis and focal necrotizing vasculitis. The combination of serial H&E sections, microCT, and synchrotron imaging showed multiple, widely open IBAs arising from pulmonary arteries and connecting with the bronchial vasculature.

Conclusion: Identifying pulmonary histopathologic correlates is necessary to better understand the pathomechanism of COVID-related severe ARF. In this study, we confirmed the presence of recruited IBAs with multiple methodologies. We propose that IBAs play a key role in COVID-related ARF by inducing precapillary right-to-left vascular shunts contributing to severe, intractable hypoxemia and death.

Novel TSPAN4-CD151 gene fusion in Wilms tumor with diffuse anaplasia

M Takeda, D Moke, G Raca, R Schmidt, R Shah, M Warren

Children's Hospital of Los Angeles, Los Angeles, California

Background: Nephroblastoma (Wilms tumor) is the most common pediatric renal malignancy. Though Wilms tumor is generally considered to have a good prognosis with a 5-year survival rate of 93%, certain histologic features are associated with poor prognosis, such as anaplasia. In addition, there are many gene alterations associated with Wilms tumor, and additional genes continue to be identified with use of molecular methods such as next generation sequencing (NGS).

Methods: We present a case of nephroblastoma (Wilms tumor) showing diffuse anaplasia with a novel gene fusion, previously unreported in the literature, including detailed clinical, histologic, and molecular pathologic findings.

Results: The patient is a 3 year old male presented with several days of hematuria. He was found to have a large renal mass and transferred to our institution for a higher level of care. On imaging, the right kidney was enlarged measuring up to 14 cm, and a large mass was identified at the lower pole, measuring 11.1 cm. The histology of the renal mass demonstrated a Wilms tumor with triphasic histologic pattern with diffuse anaplasia. The large anaplastic tumor cells and atypical mitotic figures were present in almost all of the histologic sections submitted and identified among the tumor cells in the lymphovascular invasion. Molecular studies included chromosomal microarray (CMA) which demonstrated loss of heterozygosity for 11p, 12q gain and 16q deletion, which are common alterations in Wilms tumor, and NGS which identified a *TSPAN4-CD151* gene fusion, previously unreported in Wilms Tumor. Subsequent imaging showed bilateral pulmonary nodules, which were confirmed to be metastatic Wilms tumor with diffuse anaplasia. In addition to the right nephrectomy, the patient received 6 cycles of chemotherapy including vincristine, doxorubicin, cyclophosphamide-carboplatin-etoposide (CCE).

Conclusion: We report a case of Wilms tumor with anaplasia involving a novel gene fusion, *TSPAN4-CD151*. Though the fusion has been reported in a pediatric infratentorial ependymoma, this is the first report of the fusion found in Wilms tumor. With the ever advancing personalized medicine and targeted therapies, it is important for the pathologist to continue identifying novel genetic mutations which may be actionable in the future.

Therapy-Related Acute Myeloid Leukemia Relapsing as Duodenal Myeloid Sarcoma in a Pediatric Patient with Langerhans Cell Histiocytosis.

F Alnoor¹, G Gheorghe²

¹The University of Tennessee Health Science Center, Memphis, Tennessee; ²St. Jude Children's Research Hospital, Memphis, Tennessee

Background: Myeloid sarcoma (MS) is an extramedullary neoplasm of myeloid origin. It can manifest as a de novo or therapy-related with or without bone marrow involvement. It can involve skin, bone, lymph nodes, with the gastrointestinal (GI) location being relatively uncommon in children. Concomitant Langerhans cell histiocytosis (LCH) and MS have been reported with rare reports of LCH preceding MS. In general, such cases are considered therapy-related. We report a rare occurrence of therapy-related AML relapsing as an MS in the GI tract in a patient with a history of LCH with GI involvement and emphasize the diagnostic challenges and their clinical implications.

Methods: An 8-year-old female with the past medical history of multisystem LCH involving the colon, EBV-related hemophagocytic lymphohistiocytosis, and therapy-related AML S/P matched sibling donor hematopoietic cell transplant, presented with abdominal pain. Abdominal ultrasound demonstrated a 3.5 x 2.4 x 2.2 cm intramural mass in a small bowel loop. Upper GI endoscopy showed a protruding mass in the 4th portion of the duodenum. Recurrent LCH was considered clinically because of the patient's past history of LCH with GI tract involvement. Multiple GI biopsies were submitted for pathology evaluation.

Results: The biopsy of the duodenal mass demonstrated a small bowel wall with monotonous neoplastic infiltrates involving submucosa. The tumor cells were relatively large with a high nuclear to cytoplasmic ratio, rounded to oval nuclei with fine chromatin and variably prominent nucleoli. Tumor cells were diffusely positive for CD34, CD43, CD117, and focally positive for MPO, while negative for CD3, CD20, CD1A, EBER, and langerin. CD68PGM1 was positive in a subset of cells. The morphological and immunohistochemical (IHC) findings were diagnostic of MS. Additional findings were an increased number of CD3+ intraepithelial T lymphocytes, consistent with the patient's history of GVHD. A bone marrow examination was performed and showed no morphologic evidence of leukemia or LCH. The corresponding minimal residual disease (MRD) by flow cytometry was negative. The patient received palliative care and died two months after the MS diagnosis.

Conclusion: The distinction between LCH and MS can be particularly challenging in small GI biopsies. A high index of suspicion is required to reach the MS diagnosis in a patient with a history of LCH involving the GI tract. An IHC panel to include CD34, CD117, MPO, CD68, CD43, lysozyme in addition to Langerin, CD1a, S100, should be performed. Cytogenetics and molecular testing including PCR or NGS based assays for *BRAF* V600E and myeloid neoplasm associated genes could be helpful in challenging cases. Due to the limited nature of the GI biopsy, additional ancillary studies could not be performed in our case.

Mesenchymal hamartoma of the adrenal gland in Beckwith-Wiedemann Syndrome

J Mandziuk¹, S Chan², C Sergi³, A Lacson²

¹University of Alberta, Edmonton, Alberta; ²Alberta Precision Laboratories, Edmonton, Alberta;

³Children's Hospital of Eastern Ontario (CHEO), Ottawa, Ontario

Background: Beckwith-Wiedemann Syndrome (BWS) is a genetically heterogeneous congenital overgrowth syndrome with variable expression and an increased risk of developing several types of tumors, including mesenchymal hamartoma of the liver. Mesenchymal hamartomas have been described in other locations; however, their presence in the adrenal gland has not been reported, to the best of our knowledge.

Methods: A healthy term infant of an uncomplicated pregnancy and delivery was found to have a liver lesion on prenatal ultrasound examination at 32 weeks gestation. Cystic change was evident in a portion of the placenta early in gestation with features of placental mesenchymal dysplasia confirmed on pathological examination. Post-natal MRI showed a minimally complex large cystic lesion within the right hepatic lobe favored to be a cystic mesenchymal hamartoma. The differential diagnosis included a benign hepatic cyst, hepatoblastoma, or congenital hemangioma. Additional small hypointense liver lesions were also seen, representing cysts or hemangiomas. Serum alpha-fetoprotein levels were within normal limits for age with normal liver enzymes and bilirubin. The large hepatic lesion was resected at 4 weeks of age. Follow-up imaging revealed a new complex solid-to-cystic lesion in the left adrenal gland and progressive enlargement of the remaining cystic lesions in the liver. In preparation for liver transplantation, the adrenal lesion was resected to determine its nature.

Results: The surgically resected liver lesion revealed a minimally trabeculated unilocular cyst filled with bile-stained fluid, which was determined to be a mesenchymal hamartoma of the liver, without areas of early malignancy. The surgically resected adrenal gland showed a solid lesion with a focal cystic component. Histologic findings paralleled the mesenchymal hamartoma of the liver. Puzzling, the immunohistochemistry proved the epithelial component to be adrenal in origin. Peripheral blood and adrenal tumor sample were sent for BWS testing, with the blood sample yielding a normal result and the adrenal tumor sample positive for paternal 11p15 uniparental disomy (UPD), indicative of mosaic paternal 11p15 UPD. There were no documented physical features of BWS and no family history of the same. The remaining liver lesions are presumed also to be mesenchymal hamartomas and have stabilized in size. An external consultation confirmed our diagnoses.

Conclusion: This case illustrates a unique presentation and progression of BWS-associated hamartomas. It highlights the genetic heterogeneity and variable clinical presentation of the syndrome. Additionally, we describe the characteristics of mesenchymal hamartoma of the adrenal gland for the first time. While rare, it should be included in the differential diagnosis of adrenal lesions in BWS.

Umbilical Appendix Masquerading as a Patent Omphalomesenteric Duct in a Neonate

C Karakas, P Katzman, D Wakeman, M Chacon

University of Rochester Medical Center, Rochester

Background: The umbilicus is the site of a number of well-recognized and unusual abnormalities. Well-known neonatal umbilical abnormalities include umbilical hernias, granulomas/polyps, and congenital remnants of development. Here, we report a rare case of an appendix draining through the umbilicus of a neonate. We describe this rare case along with a review of the literature and discuss the underlying pathophysiology.

Methods: The patient was an 11-week-old male infant born at 33 2/7 weeks gestation. During a 3 week NICU admission, he underwent umbilical vein catheter placement and removal due to concern for bilious drainage. After discharge, he presented at 9 weeks of age with persistent yellow-brown drainage and associated air bubbles from his umbilicus. The patient was believed to have a patent omphalomesenteric duct remnant. Two weeks later, surgical excision of this structure and umbilical exploration were performed. Upon dissection of the structure free from the umbilicus, it was noted to be a smooth walled, blindly ending piece of bowel, similar in appearance to appendix. Diagnostic laparoscopy demonstrated its origin to be the cecum, and confirmed its identity as the appendix. The infant's anatomy was otherwise normal, without signs of increased cecal mobility or malrotation. Appendectomy was performed via crush clamp technique externally. The patient recovered well after surgery.

Results: Gross examination of the specimen revealed a 5.3 x 0.4 cm appendix with a pinpoint lumen. Histologic sections showed a colonic mucosa-lined bowel wall with prominent submucosal lymphoid aggregates, that was in continuity with the umbilicus, supporting the diagnosis of an umbilical appendix.

Conclusion: Umbilical appendix is a rare condition. In the literature, only 15 cases of umbilical appendix have been recorded. The infrequent nature of the condition makes it a difficult disease to study and its pathophysiology remains incompletely understood. Embryological explanation of the etiology has been associated with either malrotation or a mobile cecum. Persistent drainage from the umbilicus that appears as urine or stool, or skin changes are important for recognition and should prompt umbilical exploration and timely treatment of this entity. Cutting off the umbilical ring with procedures such as umbilical vein catheterization, as in our patient, or clamping in suspected umbilical appendix cases may create an appendicoumbilical fistula. Although ultrasonography is helpful to rule out other underlying anomalies, surgery and the histopathology are gold standards for making the definitive diagnosis as well as treatment of the anomaly.

An Autopsy Case of a Novel ARX Mutation and Pancreatic Maldevelopment in an Infant with X-Linked Lissencephaly with Ambiguous Genitalia (XLAG)

A Moosvi, N Tatevian, M Bhattacharjee, M Covinsky

The University of Texas Health Sciences Center - Houston, Sugar Land, Texas

Background: The ARX gene, known as the Aristaless-related homeobox gene, is an approximately 12.5 kilobase pair gene located on the short (p) arm of chromosome X with five coding exons. It is expressed in multiple tissues including the pancreas, brain and testis. Null mutations are associated with X-linked lissencephaly with abnormal genitalia (XLAG). Expansions of polyalanine repeats are associated with seizures and Partington syndrome. The ARX gene has been examined in an effort to use pluripotent stem cells as a source for insulin secreting cells for transplantation. There have been many studies of the ARX gene in vitro however reports of the effects of this mutation on pancreas in human patients are rare. This is only the second report of the findings of ARX mutation in a human patient and contains unique findings.

Methods: Consent was obtained to perform a complete unrestricted autopsy examination. Tissue sections of organs were taken and processed to produce formalin-fixed paraffin-embedded tissue. Hematoxylin and eosin (H&E) stained slides from the paraffin blocks were examined. Tissue and cell blocks were then deparaffinized in xylene followed by dehydration in graded alcohol to employ immunohistochemical markers of insulin and glucagon, with appropriate controls. Slides were analyzed by board-certified pediatric pathologists and a pathology resident. Comprehensive genetic testing of the ARX gene was conducted by the medical genetics team.

Results: The pancreatic Islets of Langerhans were enlarged although hypocellular and occupied for than 50% of occasional high-power fields. An immunohistochemical stain for insulin demonstrated staining for most cells within the islets, including cells at the periphery of the islets. Furthermore, there were scattered insulin positive cells occurring singly and in clusters throughout the pancreatic parenchyma. There were instances of clusters of insulin positive cells budding off exocrine ducts. A stain for glucagon demonstrated a complete loss of staining. The ARX gene is required for the differentiation of pancreatic islet cells into glucagon producing alpha cells. We have demonstrated a case in which a mutation in ARX in a human patient blocked differentiation of islet cells into alpha cells.

Conclusion: The case presented here underlines the ARX gene and its multifaceted nature in defining endocrine pancreas cell lineage differentiation. The findings presented in our case necessitate further evaluation to elucidate the complexity of this mutational pathway on human cell lines.

A Case of Colon Carcinoma in an adolescent. A diagnostic challenge for the pediatric pathologist*K Lockart¹, D Drehner²*¹University of Central Florida College of Medicine, Haines City, Florida; ²Nemours Children's Hospital, Orlando, Florida

Background: Colon carcinoma is rare in children with an annual incidence estimated at 1 in 10 million. Pediatric patients generally present with more advanced disease than adult patients, often as a result of lack of standardized screening and limited clinical suspicion. The definitive identification of the type of colon carcinoma can have implications for family members as many cases are linked to Lynch Syndrome, an autosomal dominant hereditary disorder.

Methods: This is a case report of 16-year-old female with a five month history of abdominal pain and 5 kg weight loss..

Results: The patient recently moved to the United States from South America. A distant cousin was diagnosed with colon carcinoma in their twenties. A contrast enhanced CT of the abdomen and pelvis was interpreted as showing a large inflammatory mass immediately superior to the urinary bladder contiguous with the sigmoid colon. The origin of the mass was unclear. At surgery a large fungating mass was seen in the left lower abdomen with dense adhesions to the lateral abdominal wall. It originated from the sigmoid colon. The colon was transected 5 cm proximal and distal to the mass and sent for pathology. Bisecting the sigmoid colon segment revealed a circumferential tumor measuring 7.2 x 4.5. The colonic lumen was reduced to a pinpoint. The tumor was composed of pleomorphic cells with moderate cytoplasm and nuclei with a large distinct nucleolus. The cells were arranged in sheets and had some interspersed areas exhibiting glandular structure and other areas infiltrating in single file. The histologic features were those of a medullary type colon carcinoma. There were large areas of necrosis noted throughout the mass. There was a distinct transition from normal colonic mucosa to tumor. Neither dysplastic transition areas nor polyps were present in the resected segment. The tumor had high microsatellite instability and loss of MLH1/PMS2 protein expression by immunohistochemistry.

Conclusion: 1. The patient met three of the Bethesda Criteria for Lynch Syndrome testing- age at diagnosis, history of family member diagnosed with colon carcinoma before age 50 and the histology. However, Bethesda Criteria have a specificity of approximately 25%. 2. High microsatellite instability and loss of MLH1/PMS2 protein expression by immunohistochemistry suggest the presence of germline mutations in the MLH1 gene. The result of that testing is pending. 3. Determining appropriate measures for early detection of pediatric colonic neoplasms has proven to be a challenging endeavor when extensive family history is not available.

Diverticulum in Pediatric Crohn Disease: Case Report*J de Nanassy, C Sergi*

Children's Hospital of Eastern Ontario, Ottawa, Ontario

Background: Crohn disease has been associated with diverticulosis of small bowel and adenocarcinoma in adults, but a non-Meckel diverticulum in a child with Crohn disease has not been reported to the best of our knowledge. We present the unusual case of a diverticulum of the colonic wall arising in the context of severe ileocecal stricturing in Crohn disease.

Methods: A 15-year-old male was diagnosed with Crohn disease in August 2020. Severe stenosis at the ileocecal valve (< 3 mm, lumen diameter) was identified on colonoscopy. The fibrostenotic stricturing was unresponsive to medical therapy. Surgery was declined at that time. In June 2021, a tubular growth was detected on physical exam and ultrasound. Surgery with ileocecal resection was performed over 9 months later.

Results: Microscopy of the resected specimen showed features of Crohn disease. In addition, there was a peculiar finding of a cystically dilated diverticulum in the colonic wall adjacent to the ileocecal valve. Our interpretation is that of a diverticulum arising at a point of localized weakness in the bowel wall (such as, vessels coursing through the bowel wall, or incomplete or thin muscularis propria at the junction between terminal ileum and cecum). This colonic diverticulum would have arisen in the context of markedly increased intraluminal pressure on the bowel wall secondary to long-standing stenosis at the ileocecal junction. No other diverticula were identified.

Conclusion: According to Laplace's Law, the pressure inside an inflated container with curved surface is inversely proportional to the radius, which would explain the formation of the diverticulum close to the point of maximum stricturing. The length of time between diagnosis of the severe stricture and eventual surgery likely contributed to the formation of this unusual colonic wall diverticulum. Crohn disease patients are at risk of diverticular disease and neoplasms in adulthood and a follow-up may be required.

Embryonal Rhabdomyosarcoma (ERMS) of the Diaphragm in Basal Cell Nevus Syndrome (BCNS): A Case Report and Review of the Literature

L Berklite, O Lopez Nunez, A Bondoc, H Kim, S Bachir, K Somers, A Drach, C Talbott, A Fortener, R Nagarajan, R Hopkin, S Szabo

Cincinnati Children's Hospital Medical Center, Cincinnati, Ohio

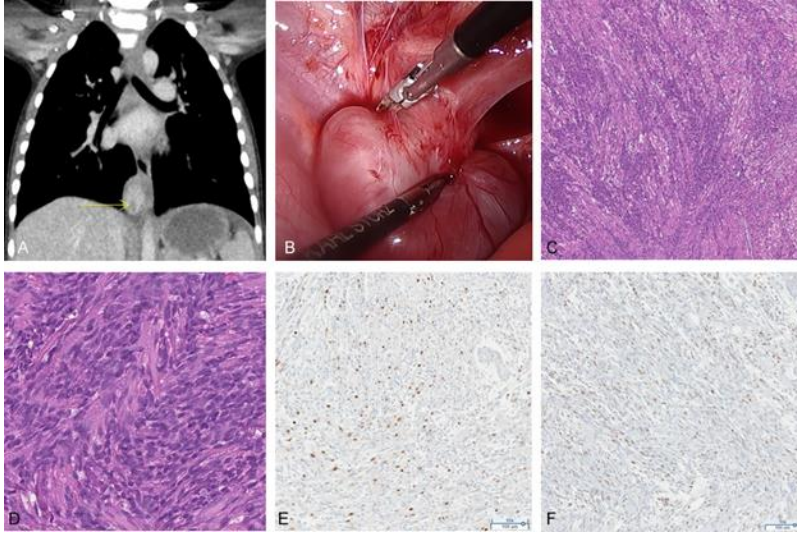
Background: Primary diaphragmatic tumors are rare and may be malignant, especially in children. We present a case of a diaphragmatic ERMS in a 4-year-old boy with a germline *PTCH1* deletion diagnostic of BCNS.

Methods: Pertinent clinical data and available pathologic material was reviewed. Our literature review focused on the diagnostic challenges presented by pediatric primary diaphragmatic malignancies and ERMS in BCNS including known molecular aberrations in patients with myogenic tumors.

Results: Our patient was a 4-year-old boy with developmental delay, hydrocephalus, Sprengel deformity, vertebral anomalies, and a spinal cyst. Genetic testing at 1 week of age included a SNP microarray and *L1CAM* sequencing; both were negative. An incidental 3.5 x 2.7 x 1.6 cm posterior mediastinal mass, found on imaging, was suspicious for esophageal duplication or bronchogenic cyst (Figure 1A). Intraoperatively, the mass was arising from the right diaphragmatic crus. Pathology revealed an ERMS with maturing rhabdomyoblasts and primitive small round cells, minimal nuclear pleomorphism, moderate mitotic activity, and no necrosis (Figure 1C). Tumor was positive for desmin (100%), MyoD1 (20-40%), and myogenin (5-25%) with a Ki67 proliferation index of 5-15%. FISH for *PAX3* and *PAX7* fusions, SNP microarray, and chromosomal analysis on tumor were negative. Focal positive margins prompted re-resection. After chemotherapy, imaging showed no evidence of disease.

Ultimately, on germline testing, whole exome sequencing revealed a *PTCH1* deletion (c.1423_1429del). Only 10 pediatric cases of diaphragmatic ERMS have been reported, none including genetic or molecular findings. While infrequent, ERMS has been reported in 7 patients with BCNS, aged 0 to 8 years, with a male to female ratio of 1.3:1. Reported associations were macrocephaly or central nervous system anomalies (3/7), skeletal anomalies (3/7), nevi (2/7), mandibular cysts (1/7), basal cell carcinoma (1/7), and an occipital fetal rhabdomyoma (1/7). ERMS locations included nasopharynx, bladder, tongue, postauricular, and paravertebral. 5 patients had *PTCH1* alterations: deletions (3/5), missense (1/5), and splice site mutation (1/5). One patient had a *PTCH2* mutation.

Figure 1. Diaphragmatic ERMS: Chest CT with contrast (A), Intraoperative photo (B), Histopathology H&E (C,D), Myogenin (E), MyoD1 (F)



Conclusion: This is the first documented case of diaphragmatic ERMS in a BCNS patient and reinforces the link between the Hedgehog signaling pathway and ERMS. Our case illustrates the clinical considerations and diagnostic difficulties in cases of ERMS in an unusual location. In particular, germline and tumor molecular testing in patients is essential to identify underlying syndromic conditions as early detection can lead to improved clinical outcomes.

A Tripartite Composite Pheochromocytoma and Ganglioneuroma with Plexiform Neurofibroma in a Patient with NF1: Case Report

M Haddad¹, L Deonarine², N Wiseman³, G Cuvelier⁴, H Shimada⁵, C Stefanovici⁶

¹University of Manitoba, Winnipeg, Manitoba; ²Dept of Pediatrics, University of Manitoba, Winnipeg, Manitoba; ³Dept Pediatric Surgery, University of Manitoba, Winnipeg, Manitoba; ⁴Cancer Care Manitoba, Winnipeg, Manitoba; ⁵Dept of Pathology, Stanford University Medical Center, Stanford, California; ⁶Dept Pathology, University of Manitoba, Winnipeg, Manitoba

Background: Composite pheochromocytoma is a rare tumour reported in the literature as a dual component tumour composed of pheochromocytoma and peripheral neuroblastic tumour (neuroblastoma, ganglioneuroblastoma, or ganglioneuroma) of neural crest origin. To date, there have not been any reports in the literature on a composite pheochromocytoma with more than two components.

Methods: We present a case of a 15-year-old male with a tripartite composite pheochromocytoma. At age three, he was diagnosed with NF1 following a diagnosis of NF1 and pheochromocytoma in several family members. He was followed-up for years for asymptomatic optic nerve and brainstem gliomas. An abdominal ultra-sound for surveillance of possible neurofibromas revealed a mass anterior and medial to the upper pole of the left kidney. By MRI, the mass, arising from the left adrenal gland and measuring 4.9x4.9x3.7cm, was well-circumscribed, with a thick and enhancing wall. Biochemical tests for pheochromocytomas were negative and the suspicion of a ganglioneuroma was made. The patient underwent surgical excision of the mass which was received for pathological examination.

Results: On gross examination, a mass arising from the adrenal gland, weighing 66 g and measuring 8.5x 5x 5.7cm, was identified. The outer surface was smooth, and the cut surface was gray-tan partially soft and partially firm, with extension beyond the adrenal gland component noted. Histological examination revealed three components: pheochromocytoma, ganglioneuroma and plexiform neurofibroma. By immunohistochemistry the tumor was positive for neurofilament in the ganglioneuroma component (ganglion cells and their neuritic processes incorporated in the cytoplasm of Schwannian stromal cells) while INSM1 highlighted the pheochromocytoma component.

Conclusion: To our knowledge this is the first case report on a tripartite composite pheochromocytoma.

Distal Villous Lesions of Placental Fetal Vascular Malperfusion Are More Frequently Higher Grade and Associated with Shorter Gestational Age and Chronic Placental Hypoxia than Those with Proximal Large Muscular Vessels

J Stanek

Cincinnati Children's Hospital Medical Center, Cincinnati, Ohio

Background: Both global and segmental fetal vascular malperfusion (FVM) feature large vessel lesions as well as distal villous lesions in their definitions. While high grade FVM is based on number of involved terminal villi and/or occluding/non-occluding thrombi in large muscular placental vessels, it is not clear if the impact of those two feature categories on perinatal outcome and placental pathology is equivalent which is the objective of this analysis.

Methods: As the recently reported distal villous FVM lesions featuring segmental endothelial fragmentation, hypovascularity, and villous mineralization identify cases with the same potential of short-term perinatal complications as cases with totally sclerotic chorionic villi seen on H&E sections only, all types of distal villous involvement were analyzed together with the numerical Amsterdam criteria for the purpose of this analysis. 479 consecutive cases of placental FVM diagnosed by the author were analyzed among 3 groups: Group 1: 86 cases with distal FVM (at least 3 or more foci of 2 to 4 terminal villi with sclerotic/hypo vascular/mineralized distal villi or villi with stromal vascular karyorrhexis seen on H&E and/or clusters of hypo vascular distal villi or mineralized villi or villi with endothelial fragmentation) without large vessel lesions; Group 2: 186 cases with large vessel lesions (fetal vascular ectasia, occluding/non-occluding thrombi, intramural fibrin deposition, stem vessel obliteration) without distal villous lesions; and Group 3: 222 cases showing both distal villous lesions and large fetal vessel lesions, i.e. combined features of FVM seen in both Group 1 and Group 2. Frequencies of 26 clinical and 38 independent placental phenotypes were statistically compared among the groups by Chi-square or analysis of variance.

Results: Statistically significant differences (p Bonferroni <0.002) were noted among Groups 1-3, respectively: average gestational age at delivery (weeks) 31 ± 7 , 35 ± 5 , 34 ± 6 , fetal growth restriction 24%, 9%, 25%, average placental weight (grams) 318 ± 167 , 413 ± 196 , 366 ± 174 , postuterine pattern of chronic hypoxic placental injury 12%, 2%, 6%, luminal vascular abnormalities in stem vessels 16%, 3%, 11%, and high grade FVM 33%, 16%, 39%. There were no significant differences in clinical umbilical cord compromise, or pathological umbilical cord abnormalities among the groups.

Conclusion: Distal FVM lesions are more frequently associated with chronic placental hypoxia, fetal growth restriction, and high-grade FVM than large vessel FVM. As the terminal villous involvement requires longer time duration for its development, it may be therefore more consequential than that of the proximal vascular lesions which are of shorter duration.

From Congenital Anomaly To Teenage Reality - A Fetal Autopsy And A Surgical Pathology Case of Obstructed Hemivagina and Ipsilateral Renal Anomaly (OHVIRA)

E Chan¹, C Stefanovici²

¹University of Calgary, Calgary, Alberta; ²University of Manitoba, Winnipeg, Manitoba

Background: Obstructed hemivagina and ipsilateral renal anomaly (OHVIRA), also known as Herlyn-Werner-Wunderlich syndrome, is a rare congenital anomaly characterized by uterus didelphys, unilateral obstructed hemivagina, and ipsilateral renal anomaly. OHVIRA has been well-documented in the medical literature, but cases of OHVIRA with pathologic descriptions are scant.

Methods: We described two cases of OHVIRA, one in a 32-gestational-week fetus and another in a 13-year-old girl.

Results: Case 1. Autopsy performed on a 32-gestational-week stillborn fetus revealed uterine didelphys, obstructed left hemivagina, and left pelvic, atrophic, duplex kidney, with both left ureters entering the obstructed left hemivagina, consistent with OHVIRA. Additional postmortem examination findings included an imperforate anus, a single right umbilical artery, and spina bifida occulta. The cause of fetal demise was probably unrelated to the congenital abnormalities, which are typically non-lethal. Rather, placental examination revealed high grade fetal vascular malperfusion, which was most likely the cause of fetal demise. Case 2. A 13-year-old girl presented with constipation and left lower quadrant pain. Ultrasound and MRI findings suggested a didelphic uterus, with a distended, blood-filled left uterine horn. A left kidney was not found. The patient underwent laparoscopy and resection of the left uterine horn, left fallopian tube, and upper vagina. Pathologic examination demonstrated left hematosalpinx and hematometra. No renal remnant was identified. The combined radiologic and pathologic findings were consistent with OHVIRA.

Conclusion: While rare, OHVIRA is well-documented as a congenital anomaly in the gynecologic, urologic, surgical, and/or radiologic literature. However, there are few surgical pathologic reports and no autopsy case reports. In addition, the association of OHVIRA, anorectal malformation, and spinal bifida have never been reported. By sharing these two cases, we hope to increase the awareness of this entity among pediatric/perinatal pathologists and help further elucidate genitourinary embryology, which is still a controversial subject.

Biliary Atresia in a Neonate with Congenital Cytomegalovirus Infection – An Autopsy Case*E Chan*

University of Calgary, Calgary, Alberta

Background: Biliary atresia (BA) is a progressive obliterative cholangiopathy of the newborn. The pathogenesis of BA is not clear, but 2 pathologic mechanisms have been proposed: (1) bile duct malformation during embryogenesis, and (2) disruption of already formed bile ducts due to cholangio-destructive effects of a virus or an autoimmune reaction triggered by a virus. A number of viruses has been implicated, but perhaps the most promising so far is cytomegalovirus (CMV), though the evidence supporting CMV as a causative agent of BA has been circumstantial.

Methods: We described an autopsy case of extrahepatic BA in a 5-day-old neonate.

Results: The mother was a 33-year-old G4P2 woman. At 20 4/7 weeks gestation (GA), ultrasound showed mildly elevated fetal abdominal circumference, with no other anomalies. The mother had an emergent c-section at 26 weeks GA due to abruption. At birth, the neonate had respiratory distress and thrombocytopenia. Infectious workup was negative. CMV IgG/IgM was not performed. Urine CMV nucleic acid test was pending. The baby's condition continued to worsen and she died on day 5 of life. An autopsy was consented. No placenta was available for examination. Autopsy revealed a premature female neonate with jaundice and mildly distended abdomen. A small amount of pleural, pericardial, and peritoneal bilious fluid was present. All organs had a yellow tinge. The liver and gallbladder were of normal size and shape. Clear biliary fluid was noted in the gallbladder lumen. Examination with the aid of a dissecting microscope revealed an atretic common hepatic duct. Microscopically, CMV immunopositive inclusions were present in almost all organ tissues. In particular, many CMV inclusions were present in the bile duct epithelium, causing bile duct injury. The mother's blood (collected at time of delivery) was CMV IgG +ve and IgM -ve. In light of the autopsy findings, the mother's stored prenatal blood sample (collected at 9 5/7 weeks GA) was tested; it was positive for CMV IgG, IgM, and showed low IgG avidity.

Conclusion: A meta-analysis study had shown that approximately 25% of infants with BA had evidence of CMV infection by viral PCR, culture, and/or antigen detection. However, there have only been rare pathology case reports showing an association between CMV and BA. This is perhaps the first case demonstrating concomitant CMV inclusions in the bile duct epithelium, bile duct injury, and BA. Test results of the stored prenatal (1st trimester) maternal blood sample indicated that the mother likely acquired CMV around the time of conception. Given that the gallbladder was normally sized and shaped, congenital CMV infection likely did not affect the embryogenesis of the gallbladder and biliary tree. Rather, CMV likely damaged the bile ducts after the bile ducts were fully formed.

Bilateral Schizencephaly and Dandy Walker Malformation with Accompanying Bile Duct Malformation: Case Report

S Ikegami¹, J Lee², L Ernst²

¹University of Cincinnati, Department of Pathology, Cincinnati, Ohio; ²NorthShore University HealthSystem, Department of Pathology, Evanston, Illinois

Background: Schizencephaly is a rare congenital cortical malformation, characterized by abnormal clefts in the cerebral hemispheres extending from the lateral ventricle to the cerebral cortex. Although schizencephaly is often associated with other brain malformations, concomitant other systemic anomalies have not been described in detail. We report a case of bilateral schizencephaly, Dandy-Walker malformation and hepatic bile duct malformation identified at autopsy in a 23 week gestation age stillborn fetus delivered to a G4P2 female.

Methods: Complete autopsy including placental examination and chromosomal microarray analysis were performed.

Results: Autopsy revealed a non-macerated 23 weeks gestational age female fetus with growth and maturation appropriate for gestational age. The brain demonstrated cystic dilatation of bilateral lateral ventricles with missing portions of frontoparietal lobe, parietotemporal lobe, and insula. The only remaining tissues were cystic membranes lined by abnormal gray matter. Abnormal nodularity/polymicrogyria was noted in the remaining frontal lobes. Dandy-Walker malformation and acute anoxic-ischemic changes were also identified. In addition, there was hepatic ductal plate malformation characterized by the retention of embryonic bile duct structures along the edges of the portal tracts without the well-formed interlobular bile ducts. No cytogenetic abnormality was seen in the microarray analysis of the fetus. The placental examination revealed appropriate weight placenta for 23 weeks gestational age with high-grade fetal vascular pathology. No definitive evidence of infection was present.

Conclusion: Schizencephaly is differentiated from hydrocephalus by the features of a migrational disturbance, such as large neuronal heterotopias bordered by adjacent polymicrogyria on histologic examination. The autopsy uncovered schizencephaly, as well as additional systemic anomalies including a hepatic ductal plate malformation. The underlying etiology of schizencephaly in this case is not certain because of the coexistence of two different features; 1) the abnormal gray matter lining the cysts and the frontal lobe nodularity of the fetal brain support a primary migrational disorder; 2) the loss of brain tissue in the distribution of the middle cerebral arteries supports vascular disruption as the primary etiology. Given the abnormal placental pathology in addition to the normal microarray result, vascular disruption during critical times in utero may have contributed to disturb fetal development, and ultimately lead to a wide range of anomalies including the abnormal neuronal migration, cerebellar vermis hypoplasia, and intrahepatic bile duct development arrest. This case demonstrates how critical the intrauterine environment can be for fetal organ development.

Outcomes of Giant (≥ 10 cm) Cord Hemangiomas: Case Report and Literature Review

E Ferreira¹, R Govia², J Hunt², C Stefanovici¹

¹Department of Pathology, University of Manitoba, Winnipeg, Manitoba; ²Department of Obstetrics, Gynecology & Reproductive Sciences, Winnipeg, Manitoba

Background: Umbilical cord (UC) hemangiomas are rare lesions often presenting with striking clinical and/or ultrasonographic findings. Giant (≥ 10 cm) UC hemangiomas are exceedingly rare, hence prognostic information is lacking.

Methods: We present a case of a 36-year-old G1P0 mother diagnosed by ultrasound with a 12cm vascular UC mass. She was closely followed and delivered a healthy infant (APGAR score 9 at 1&5 minutes) via caesarean section at 37-weeks. Pathologic examination of the placenta along with a Pubmed search of the English-language literature using search terms “umbilical cord hemangioma” OR “umbilical cord angiomyxoma” was performed.

Results: On gross examination, the UC was massively distended by a 11.5x5.0x4.0cm tumor located 49cm from disc insertion. Sectioning revealed marked edema and cystic-type change of the Wharton jelly. Histologic examination confirmed giant UC hemangioma originating from an umbilical artery. The endothelial cells were CD34-immunoreactive while negative for Glut-1 and D2-40, which ruled out chorangiotic and lymphatic origins, respectively. Pubmed search yielded 44 previous UC hemangioma cases, of which 7 were ≥ 10 cm. Six of 7 cases were complicated by hydrops, congenital heart disease, respiratory distress and/or demise. Of the 37/44 cases < 10 cm, 22 yielded healthy infants while 15 reported major complications similar to those of giant hemangiomas.

Conclusion: This is the second reported case of a giant UC hemangioma that resulted in a healthy infant. Systematic literature review yielded information limited to case reports with no clear association to aneuploidy or specific syndromes. Due to high risk of major adverse outcomes, these lesions require close monitoring antenatally.

Case Report of Ivemark Syndrome in a Male Neonate

C Bockoven, R Mahabir, P Wong, M Warren, L Szymanski

Children's Hospital Los Angeles, Los Angeles, California

Background: Laterality disorders develop due to a failure establishing normal left to right symmetry. Ivemark syndrome is a rare laterality disorder that consists of a constellation of findings including right atrial isomerism with atrial appendages of the morphologic right type and asplenia. Half of the time the liver is symmetric with the stomach, duodenum and pancreas on the right side with variability in the degree of intestinal malrotation. There is no known cause and is usually sporadic with rare reports of it affecting multiple family members. Although multiple genes have been identified for important roles with heterotaxy, no specific gene has been definitively linked to this syndrome. Laterality disorders overall affects an estimated 1 in 15,000 people. The exact incidence of Ivemark syndrome is unknown. We report here a case of Ivemark syndrome with significant cardiac malformations.

Methods: Patient information was gathered from the electronic medical record and prior pathology records. Autopsy was requested by family and consent was obtained for a complete unrestricted autopsy. Routine and immunohistochemical stains and electron microscopy were performed on the postmortem tissue. The cardiorespiratory exam was done along with a pediatric cardiologist.

Results: A male neonate was delivered to a G5P4 mother at 39 weeks gestation. Prior prenatal screening identified a complex congenital heart defect leading to immediate transfer to the pediatric hospital at birth. During hospitalization he had 4 cardiopulmonary arrests resulting in multiorgan failure, profound acidosis, and severe electrolyte derangement. Despite care he passed away at 3 days of life. Autopsy findings showed a well-developed male neonate with gross features consistent with heterotaxy with a complex congenital heart defect. Grossly the abdominal cavity showed the stomach located on the right side, absence of the spleen, midline liver with the gallbladder on the left side of the liver, pancreatic hypoplasia and intestinal malrotation. The lungs showed right-sided patterning with both lungs containing three lobes with epiarterial bronchi. The heart was located in normal position however there was transposition of the great arteries and total anomalous pulmonary venous return. The aortic arch curved to the right with hypoplastic segments, mirror image branching of the arch vessels and a large right-sided ductus arteriosus. There was no innominate vein but bilateral superior vena cavae.

Conclusion: Recognizing laterality defects is important as well as searching for associated congenital malformations. Identifying a particular laterality syndrome is useful as some disorders including Ivemark syndrome are rare. Good documentation of these case might lead to better understanding of this rare groups of syndromes in the future.